Institute of Meteorology and Climatology
Gottfried Wilhelm Leibniz Universität Hannover

Report

# Evaluation of the PALM model system according VDI 3783 Part 9

from
Dipl.-Met. Viola Weniger

August 2019

# Contents

# 1 Introduction

This report evaluates the parallelized LES model PALM using the guideline VDI 3783 Part 9. This guideline refers to prognostic micro-scale wind field models and is used for the evaluation of building and obstacle flow. A model is considered as evaluated if the following items are fulfilled:

- general evaluation (chapter 2)
- scientific evaluation (chapter 3)
- validation (chapter 4)
- internal assessment (chapter 5).

# 2 General evaluation

The general assessment includes the following items:

**Comprehensibility**
The model PALM is comprehensible by third parties. A documentation of the model and the program can be found on the PALM homepage (*https://palm.muk.uni-hannover.de/trac*). Also the inspection of the source code is possible for third parties and there are several publications of the model physics and its results [Maronga *et al.* (2019), Schwenkel und Maronga (2019), Gronemeier und Sühring (2019), Kanani-Sühring und Raasch (2017), Knoop *et al.* (2019), Maronga *et al.* (2015)].

**Brief description**
A brief description of PALM can be found in Maronga *et al.* (2019).

**Detailed model description**
A detailed model description, where the fundamental equations, approximations, parameterisations and boundary conditions are listed can be found at *http://palm.muk.uni-hannover.de/trac/wiki/doc/tec.*
The application limits, further developments of the model and references to the literature are listed at *http://palm.muk.uni-hannover.de/trac/wiki/doc/tec/releasenotes* and the units of the parameters at *http://palm.muk.uni-hannover.de/trac/wiki/doc/app/parlist.*
**Manual**
Informations about the installations procedure and the hard- and software requirements are described at *http://palm.muk.uni-hannover.de/trac/wiki/doc/install.* The Description of the input data (*http://palm.muk.uni-hannover.de/trac/wiki/doc/app/inipar*) and output data (*http://palm.muk.uni-hannover.de/trac/wiki/doc/app/d3par*), the meaning of the error messages (*http://palm.muk.uni-hannover.de/trac/wiki/doc/app/errmsg*) and some application examples (*http://palm.muk.uni-hannover.de/trac/wiki/doc/tut/palm#Lecturepresentations*) can also be found on the PALM homepage.

**Technical reference**
The source code of PALM is disclosed. Third parties have the option to look and change the source code after installation. The source code of the PALM model system 6.0 is available at *http://palm.muk.uni-hannover.de/trac/browser/palm/tags/release-6.0.*

# 3 Scientific evaluation

The PALM model system fulfills the following required properties:

- all three wind components are prognostic
- continuity equation complete of inelastic approximation
- fluxes continuous as a function of the location
- fluxes continuous as a function of the stratification
- direct computation of the near-ground fluxes of wall functions
- symmetry of the shear tensor
- buildings resolved explicitly
- building roughness taken into account

and the application-dependent properties:

- stratification non-neutral: temperature prognostic
- stratification non-neutral: specific humidity prognostic
- stratification non-neutral: buoyancy forces (e.g. Boussinesq approximation)
- stratification non-neutral: turbulence parameters a function of stability
- No near-ground winds for initialisation: Coriolis force taken into account
- terrain gradient $>$ 1:20: orography taken into account explicitly
- 3D non-equidistant grid .

# 4 Validation

## 4.1 Description of the methods and specifications for the simulations

All calculations are carried out with the revision 4113 of PALM. In addition, the file `vdi_internal_controls.f90` containing the internal controls has been added to the `SOURCE` directory.
All simulations are preformed in the RANS mode. This means that the Reynolds-averaged Navier-Stokes equations are solved and the turbulence is completely parametrized. As parametrization for the turbulent diffusion coefficient $K_m$ the Prandtl-Kolmogorow relation [Kolmogorow (1942) and Prandtl (1945)] is used in all test cases (`turbulence_closure = 'TKE-l'`). Also cyclic boundary conditions are assumed at the edges of the model area in all simulations. At the top Neumann boundary conditions are used for the horizontal wind components.

### 4.1.1 Calculation of the initial wind profile

By default, PALM simulates the atmospheric boundary layer with Coriolis force. The input profiles are initialized by using the geostrophic wind. In some of the following test cases the Coriolis force should be neglected. For these cases, the model can not be driven by specifying the geostrophic wind. It is necessary to perform the simulations by specifying an external pressure gradient $D_i$. In these cases the vertical profile of the horizontal wind $\bar{u}_i$ is described by [Letzel (2007)]:

$$\bar{u}_i(z) = \bar{u}_i\left(z_{ref}\right) + \frac{D_i}{2\tilde{K}_m}\left(z - z_{ref}\right)\left(n(z_{top} - z_{ref}) - (z - z_{ref})\right) . \tag{4.1}$$

There $z_{top}$ is the height of the model boundary, $z_{ref}$ is the height of the normalization point $P_{Norm}$, $\tilde{K}_m$ is the turbulent diffusion coefficient and the parameter $n$ describes the type of the flow. $n = 1$ signifies a channel flow and $n = 2$ a free stream flow.

### 4.1.2 Specifications for grid spacing and model area size

In simulations with buildings some requirements about the grid must be taken into account. In the vertical a fine resolution must be simulated up to a height of twice the tallest building in the simulation area. The grid must include at least twelve levels up to

this height. Furthermore, the vertical grid spacing should be less than 10 m in the area of the buildings. Also the buildings should be resolved with at least three grid points [VDI 3783 Bl. 9 (2017)].
When choosing the size of the model area, it should be noted that the area in horizontal and vertical has such a large extent that independence of the model results from the model upper limit and the horizontal extent can be guaranteed. One criterion for this is the blockage ratio $\Phi$. This considers the ratio of built-up area $A_{\text{built-up area}}$ to total cross-sectional area $A_{\text{model area}}$. These surfaces are to be determined perpendicular to the direction of flow. For the blockage ratio the following holds [VDI 3783 Bl. 12 (2000)]:

$$\Phi = \frac{A_{\text{built-up area}}}{A_{\text{model area}}} < 10\,\% \ . \tag{4.2}$$

This criterion is fulfilled for all test cases.

### 4.1.3 Consideration of different roughness lengths

In the test cases with buildings, different roughness lengths are specified for the floor and the building walls. In the used version of PALM a specification of the roughness length is not possible in the parameter file. For this reason, the file `user_module.f90` (Subroutine `user_init`) has been modified.
Here, on the one hand, the roughness of the building walls for the four cardinal directions was set to the given roughness length. On the other hand, the roughness was considered separately for surfaces aligned parallel to the ground. Computing surfaces located on the ground get the specified ground roughness. For all other surfaces, the roughness for walls is used.

## 4.2 Description of the evaluation methods

### 4.2.1 Evaluation of the model results

An evaluation of the model results takes place on the basis of the hit rate $q$, which results of the total number correctly predicted values $n$ and the total number of comparison values $N$ [VDI 3783 Bl. 9 (2017)]:

$$q = \frac{1}{N} \sum_{i=1}^{N} n_i \tag{4.3}$$

with

$$n_i = \begin{cases} 1 \text{ if } \left| \dfrac{P_i - O_i}{O_i} \right| \leq D \text{ or } |P_i - O_i| \leq W \\ 0 \text{ else} \end{cases} \tag{4.4}$$

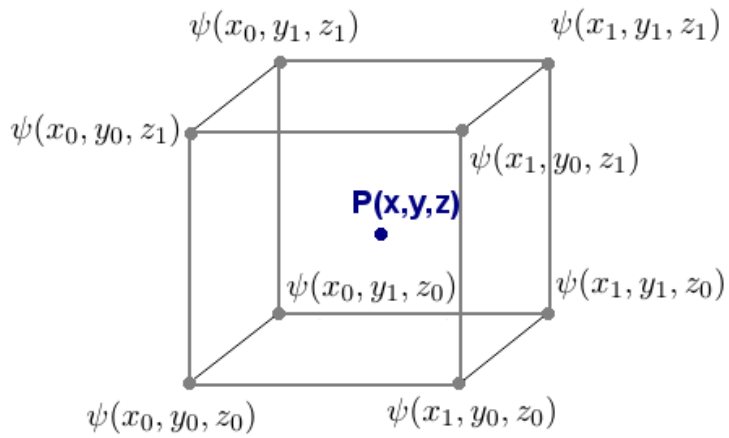


Figure 4.1: Schematic representation of trilinear interpolation.

$P_i$ describes the normalized model results and $O_i$ the normalized comparison values. The values for the permitted absolute difference $W$ and the permitted difference $D$ are given for each test case. A test is passed if the calculated hit rate is greater than the specified hit rate.

### 4.2.2 Trilinear interpolation

For a comparison with the available wind tunnel data, for the determination of the meteorological quantities $u$, $v$, $w$ and $K_m$ at the normalization point $P_{Norm}$ and for the transformation of the quantities on a rotated grid (see, e.g. test case a5), the quantities (described in the following equations by $\psi$) have to be interpolated. For this the trilinear interpolation is used.
In this method, the relative distance from point P(x,y,z) to the surrounding grid points, where the variable $\psi$ is defined, is determined (see Fig. 4.1):

$$x_d = \frac{x - x_0}{x_1 - x_0}, \quad y_d = \frac{y - y_0}{y_1 - y_0}, \quad z_d = \frac{z - z_0}{z_1 - z_0} \ . \tag{4.5}$$

Afterwards, it will be interpolated in $x$-direction:

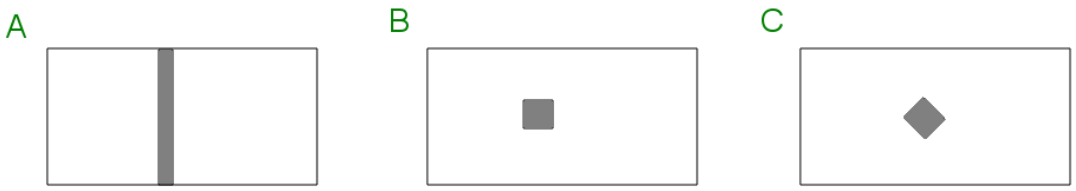


Figure 4.2: Sketches of the different building configurations of the test cases a.

$$\begin{aligned}
\psi_{00} &= \psi(x_0, y_0, z_0) \cdot (1 - x_d) + \psi(x_1, y_0, z_0) \cdot x_d \\
\psi_{01} &= \psi(x_0, y_0, z_1) \cdot (1 - x_d) + \psi(x_1, y_0, z_1) \cdot x_d \\
\psi_{10} &= \psi(x_0, y_1, z_0) \cdot (1 - x_d) + \psi(x_1, y_1, z_0) \cdot x_d \\
\psi_{11} &= \psi(x_0, y_1, z_1) \cdot (1 - x_d) + \psi(x_1, y_1, z_1) \cdot x_d
\end{aligned} \tag{4.6}$$

then in $y$-direction:

$$\begin{aligned}
\psi_0 &= \psi_{00} \cdot (1 - y_d) + \psi_{10} \cdot y_d \\
\psi_1 &= \psi_{01} \cdot (1 - y_d) + \psi_{11} \cdot y_d
\end{aligned} \tag{4.7}$$

and finally in the vertical:

$$\psi_{P_{x,y,z}} = \psi_0 \cdot (1 - z_d) + \psi_1 \cdot z_d \ . \tag{4.8}$$

The variable $\psi_{P_{x,y,z}}$ describes the value of $\psi$ at the point $P_{x,y,z}$.

## 4.3 Test cases

### 4.3.1 Overview of the individual test cases

| Test case | Description | Test | Model area (see Fig. 4.2) | Passed? |
|---|---|---|---|---|
| a1-1 | Test of the two-dimensionality: orthogonal flow of a building extending over the whole model area | homogeneous conditions in y-direction for $u$, $w$ und $K_m$ | A | yes |
| a1-2 | Test of scalability: test case a1-1 with different wind speed | Match of the normalized fields of $u$ and $w$ from test case a1-1 and a1-2 | A | yes |
| a2 | Test of integration time independence: test case a1-2 with at least twice the integration step | Match of the fields of $u$ and $w$ from test case a1-2 and a2 | A | yes |
| a3-1 | Test of the length of the wake vortex: use simulation a1-2 | Length of the wake must be between 4·H and 5·H | A | yes |
| a3-2 | Test of the length of the wake vortex as a function of the turbulence: reduction of the roughness length | length of the wake is greater than in a3-1 | A | yes |
| a4-1 | Test of symmetry: flow of a square building | symmetric fields of $u$, $w$ and $K_m$ | B | yes |
| a4-2 | Test of the dependence of the results on the grid spacing: simulation a4-1 with half grid spacing in $x$-, $y$- and $z$-direction | Match of the fields of $u$, $v$ and $w$ from test case a4-1 and a4-2 | B | yes |
| a5 | Test about building alignment in the grid: simulation with flow from 225° and grid parallel aligned building and simulation with flow from 270° and 45° rotated building | Match of the fields of $u$, $v$ and $K_m$ | C | yes |

Table 4.1: Overview of the test cases a

| Test case | Description | Test | Passed? |
|---|---|---|---|
| b-1 | Test of the horizontal homogeneity and of the simulation accuracy: simulation without building, wind direction: 0° | homogeneity of the profiles of $u$-, $v$- and $K_m$ and Match of the $u$ profile with the logarithmic wind profile | yes |
| b-2 to b-6 | Test about the effect of the approach direction of flow: test case b-1 with wind direction 32.3° (b-2), 45° (b-3), 90° (b-4), 180° (b-5) and 270° (b-6) | Match of the fields of $u$, $v$ and $K_m$ from test case b-2 till b-6 with b-1 | yes |
| b-7 | Test about the effect of the Coriolis force: simulation b-1 with Coriolis force | Match of the rotation angle (calculated by the results of b-1 and b-7) with the analytical solution (10° deviation allowed) | yes |
| b-8 to b-12 | Test about the effect of the Coriolis force and the approach direction: test case b-7 with wind direction 32.3° (b-8), 45° (b-9), 90° (b-10), 180° (b-11) and 270° (b-12) | Match of the fields of $u$, $v$ and $K_m$ from test case b-8 till b-12 with b-7 | yes |

Table 4.2: Overview of the test cases b

| Test case | Description | Test | Passed? |
|---|---|---|---|
| c1 | see test case a1-2 | Match of the fields of $u$ and $w$ from test case a1-2 with wind tunnel data | yes |
| c2 | see test case a4-2 | Match of the fields of $u$, $v$ and $w$ from test case a4-2 with wind tunnel data | yes |
| c3 | see test case a5-1 | Match of the fields of $u$, $v$ and $w$ from test case a5-1 with wind tunnel data | yes |
| c4 | simulation of a flow around a cuboid building | Match of the fields of $u$, $v$ and $w$ from test case c4 with wind tunnel data | yes |
| c5 | simulation of a flow in a area with complex buildings | Match of the fields of $u$ and $v$ from test case c5 with wind tunnel data | yes |

Table 4.3: Overview of the test cases c

### 4.3.2 Test case a1-1: two-dimensionality

In the test case a1-1 the two-dimensionality of the model results is tested. For this, the flow across an in the y-direction elongated building (see Fig. 4.2, A) is simulated. If two-dimensionality is fulfilled, the results for the zonal wind $u$, the vertical wind component $w$ and the turbulent diffusion coefficient $K_m$ must be homogeneous in the y-direction in the context of the model inaccuracy. The model inaccuracy is checked according to section 4.2.1. The hit rate to be achieved is 95% for all three quantities.
The input and simulation parameters used in this test case are listed in table 4.4. The size of the model area and the grid spacing fulfilled the specifications required in section 4.1.2. The calculation of the initial profile is described in section 4.1.1. In this connection $\tilde{K}_m = 18$ m$^2$/s is used.
Figure 4.3 shows the time series of the total kinetic energy of the flow $E$, the horizontally average of the friction velocity $u^*$ and the maximum of the $u$-component of the velocity $u_{max}$. All quantities have a constant value at the end of the simulation. This fulfills the requirement for stationarity.
The vertical profile of $u$ is shown in Fig. 4.4 for different times. From time $t = 14400$ s, only a slight change can be seen in the values. At this time, the wind speed corresponds with 10.08 m/s at the normalization point the required wind speed.
The horizontal and vertical distributions of the comparison variables $u$, $w$ and $K_m$ are shown in Figs. 4.5 and 4.6 for t = 36000 s. These are time averaged values (7200 s average). In the xy-sections, a homogeneous distribution can be seen in the y-direction. This homogeneity can also be found in the other vertical levels.
The hit rate of the quantities is 100 %. There the values of all grid points in the model area ($x_i$, $y_i \neq 0$, $z_i$) are compared with the values on the symmetry axis ($x_i$, $y_i = 0$, $z_i$).
**⇒ Test case passed**

| | |
|---|---|
| **model area** | |
| grid points | $nx = 335$<br>$ny = 83$<br>$nz = 64$ |
| grid spacing | $dx = 2.5$ m<br>$dy = 2.5$ m<br>$dz = 2.5$ m (for $z \leq 37.5$ m)<br>$dz_{k+1} = dz_k \cdot 1.08$ (for $z > 37.5$ m)<br>$dz_{max} = 20$ m |
| extension | $-230$ m $\leq x \leq 607.5$ m<br>$-105$ m $\leq y \leq 102.5$ m<br>0 m $\leq z \leq 714.5973$ m |
| **building** | |
| building dimensions<br><br><br>position of the centre: | $H = 25$ m<br>$L = 25$ m<br>$B = 207.5$ m<br>$x = 0$ m, $y = 0$ m |
| **simulation parameter** | |
| simulation period:<br>averaging period: | 10 hours<br>2 hour |
| **meteorology** | |
| wind direction:<br>wind speed at $P_{Norm}$:<br>pressure gradient:<br>Coriolis force: | 270°<br>10 m/s<br>$D_x = -0.0015$ Pa/m, $D_y = 0.0$ Pa/m<br>no |
| **further parameter** | |
| roughness:<br>normalization point $P_{Norm}$: | ground: 0.1 m, walls 0.01 m<br>$x = -70$ m, $y = 0$ m, $z = 75$ m |

Table 4.4: Input parameters of test case a1-1

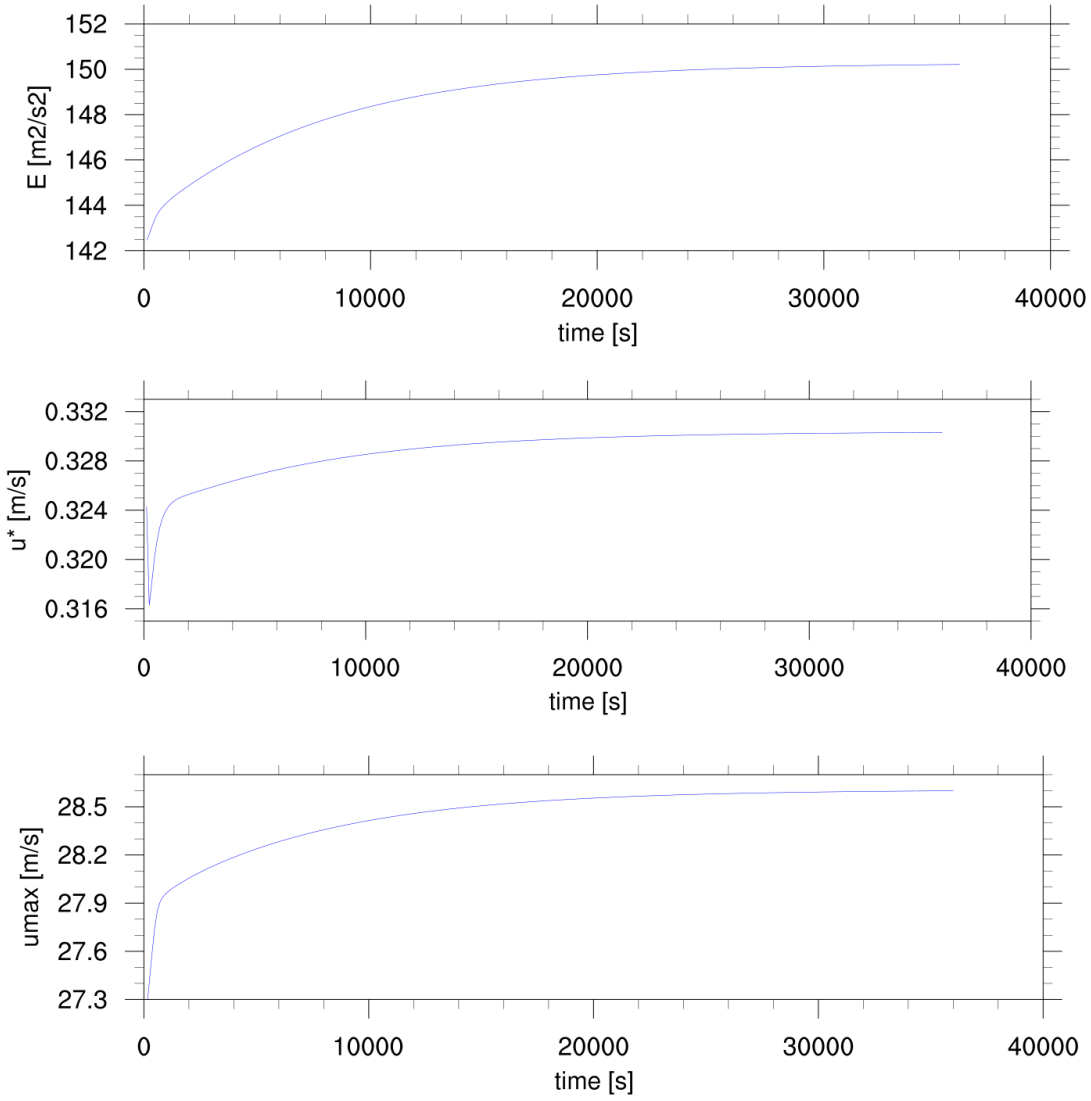


Figure 4.3: Time series of $E$, $u^*$ and $u_{max}$ for test case a1-1.

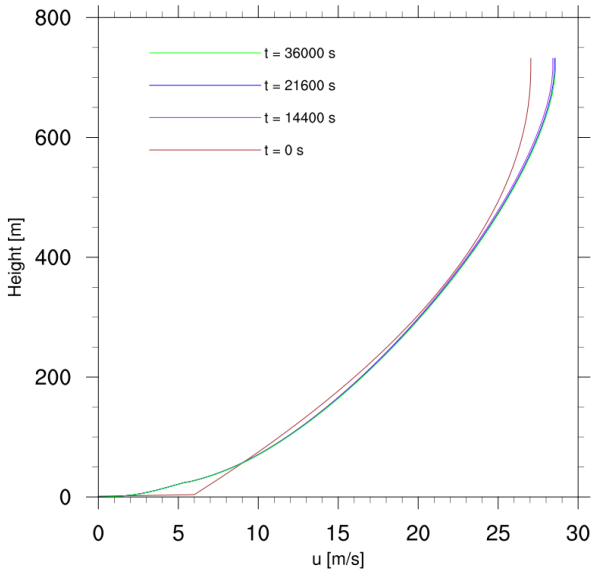


Figure 4.4: Horizontally averaged vertical profile of $u$ at $t = 0$ s, $t = 14400$ s, $t = 21600$ s and $t = 36000$ s for test case a1-1.

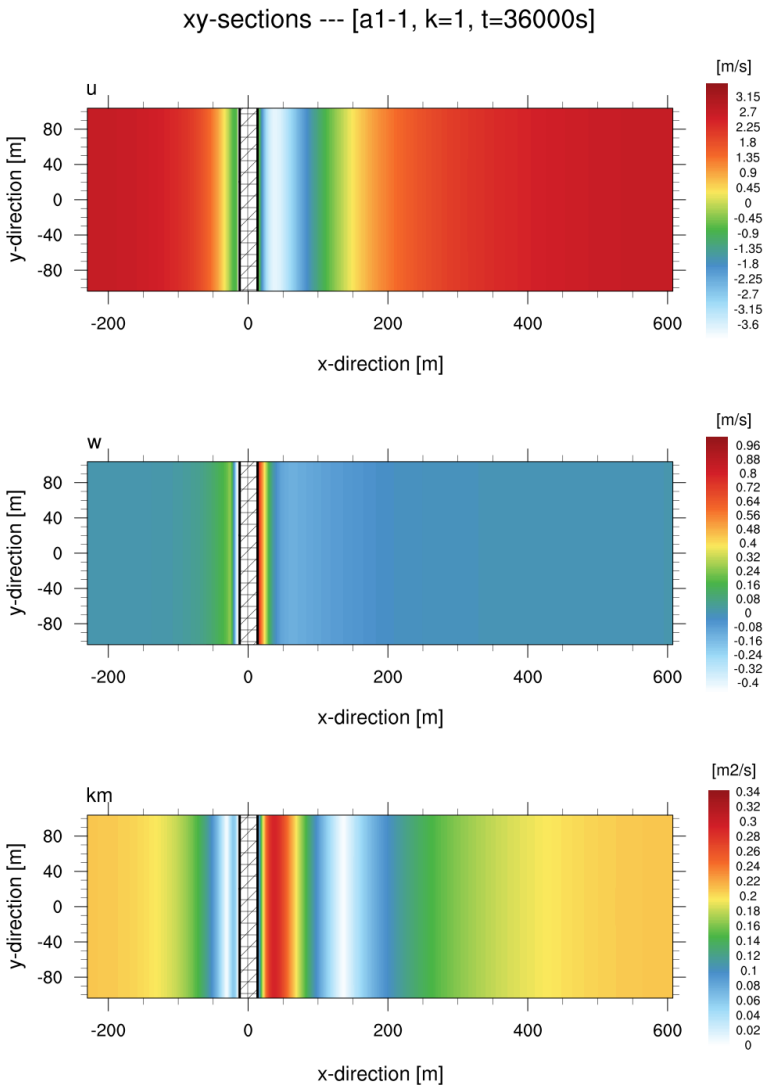


Figure 4.5: xy-sections of $u$ (m/s), $w$ (m/s) and $K_m$ $(m^2/s)$ at $k = 1$ and $t = 36000$ s for test case a1-1.

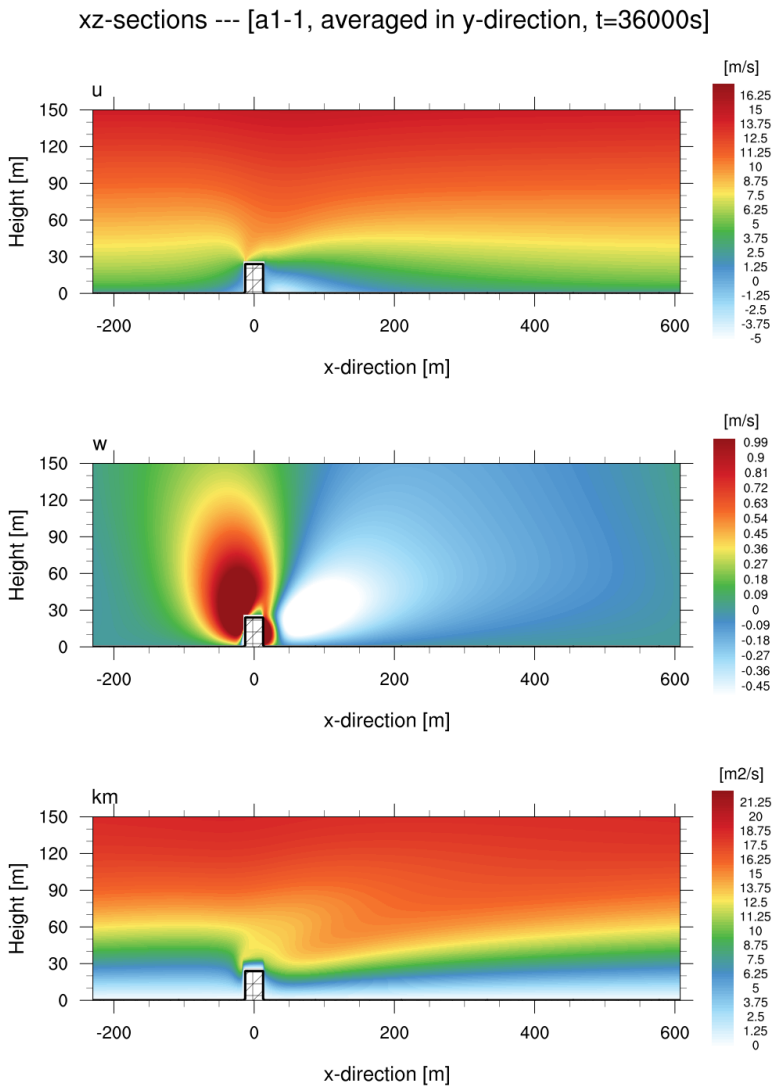


Figure 4.6: Horizontally averaged xz-section of $u$ (m/s), $w$ (m/s) and $K_m$ $(m^2/s)$ at $t = 36000$ s for test case a1-1.

### 4.3.3 Test case a1-2: scalability

In this test case, the independence of the results from the flow velocity is to be tested. For this purpose, the flow from test case a1-1 is reduced from 10 m/s to 1 m/s in 75 m height. Therefor, a pressure gradient of 0.000017 Pa/m is used in the $x$-direction. The simulation duration is 80 hours and the averaging period is two hour. The other settings are the same as test case a1-1 (see tab. 4.4).
Figure 4.8 shows the vertical profile of $u$ for different time periods. From $t = 144000$ s a barely noticeable change in the wind is observed. At time $t = 288000$ s, the wind speed at the normalization point is 1.06 m/s.
To determine the hit rate, the normalized values of $u$ and $w$ at all grid points in the plane of symmetry up to a height of 75 m are compared with those of test case a1-1. In the horizontal, the comparison plane extends from 37.5 m on the windward side of the building to 187.5 m in the lee. The hit rate is 100 % for $u$ and $w$.
⇒ **Test case passed**

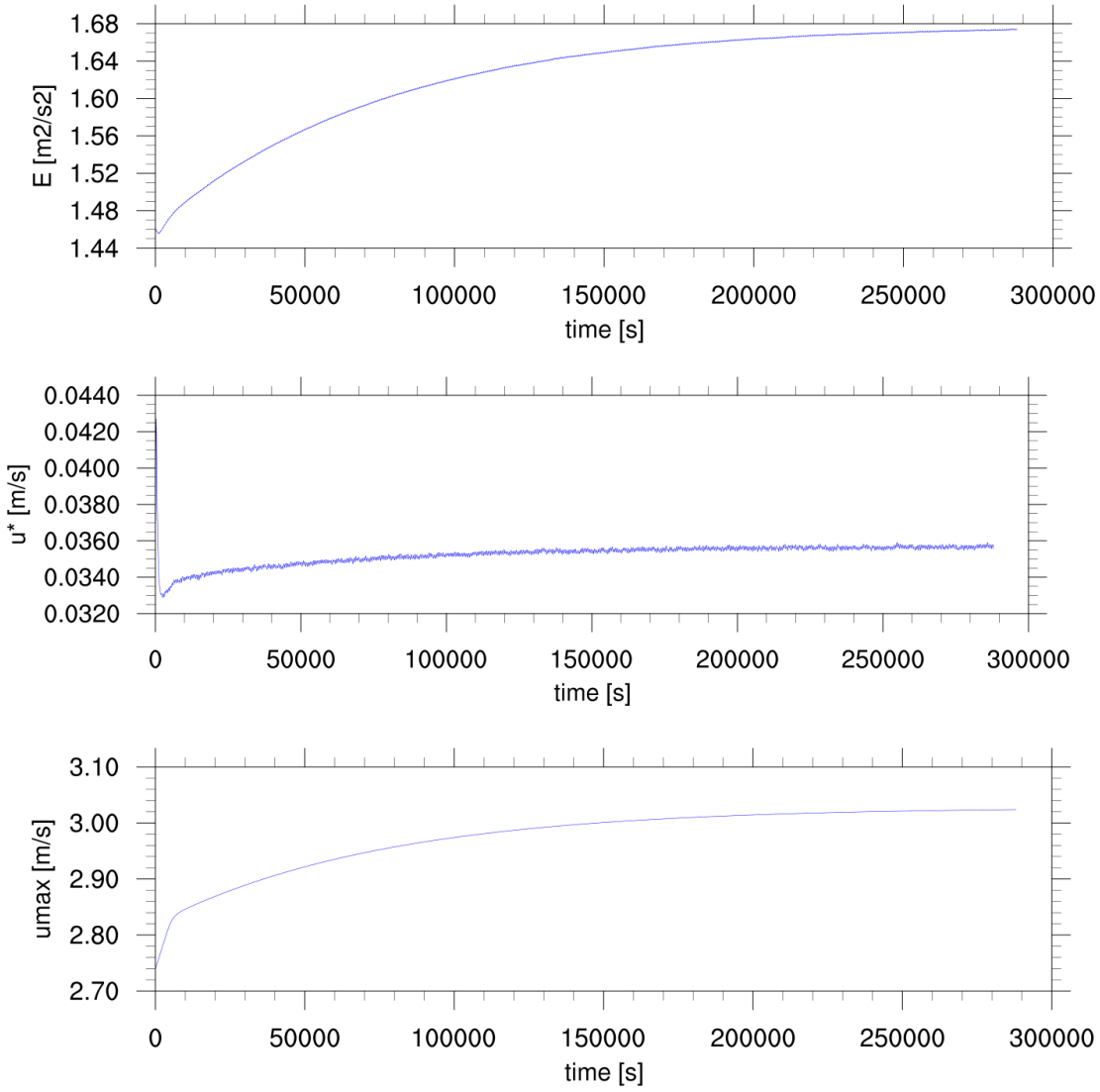


Figure 4.7: Time series of $E$, $u^*$ and $u_{max}$ for test case a1-2.

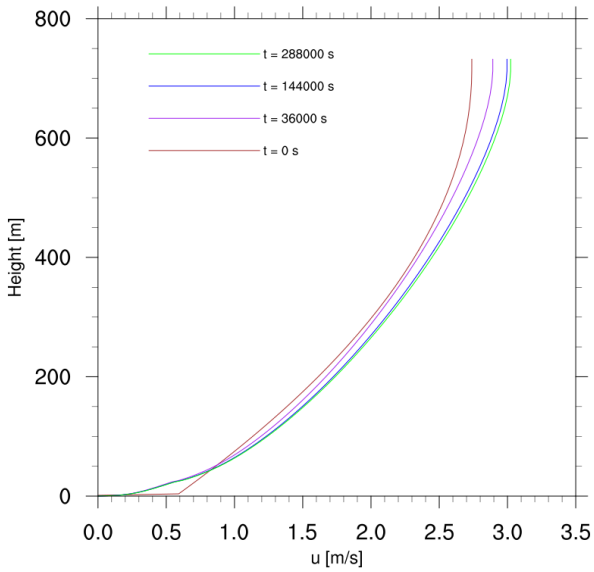


Figure 4.8: Horizontally averaged vertical profile of $u$ at $t = 0$ s, $t = 36000$ s, $t = 144000$ s and $t = 288000$ s for test case a1-2.

### 4.3.4 Test case a2: stationarity

In this test case, the independence of the model results from the number of integrations should be tested. For this purpose, the simulation of test case a1-2 should be carried out with at least twice the number of time steps, whereby it should be more than 1000 integration steps.
In test case a1-2, the number of time steps at time $t = 288000$ s is 1234966. In test case a2, 3803197 integration steps are preformed with a simulation time of 180 hours. The time series of $E$, $u^*$ and $u_{max}$ are shown in Fig. 4.9.
For the evaluation of the test case, the quantities $u$ and $w$ should be compared with each other. The hit rate is in comparison of the $u$-components 99.21 % and 100 % for the $w$-components. So the rate is above the required 95 %. As in test case a1-2, the quantities are compared at all grid points of the plane of symmetry up to a height of 75 m and 37.5 m on the windward site and 187.5 m in the lee of the building. The wind speed at the normalization point is 1.06 m/s in both cases.
$\Rightarrow$ **Test case passed**

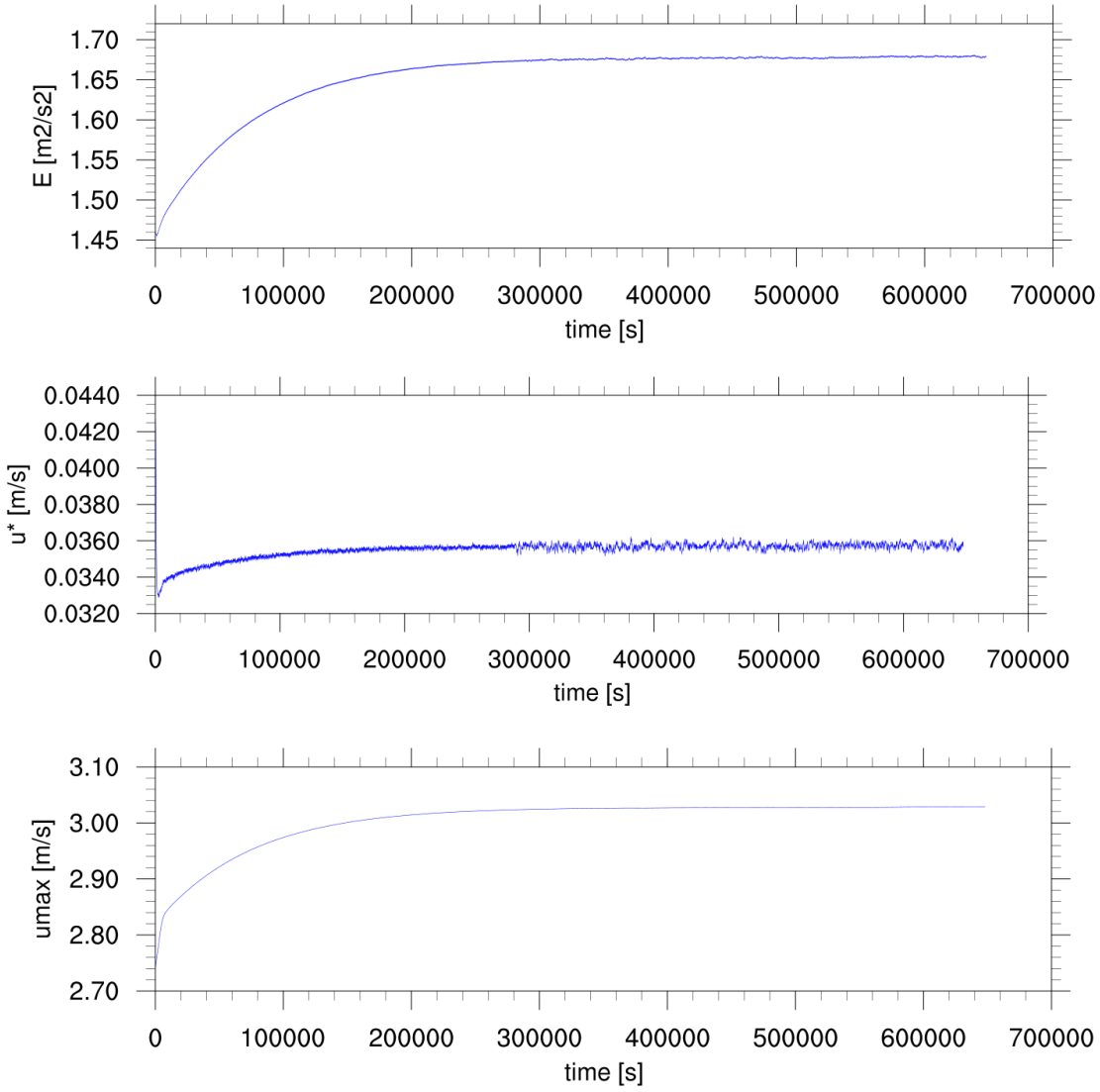


Figure 4.9: Time series of $E$, $u^*$ and $u_{max}$ for test case a2.

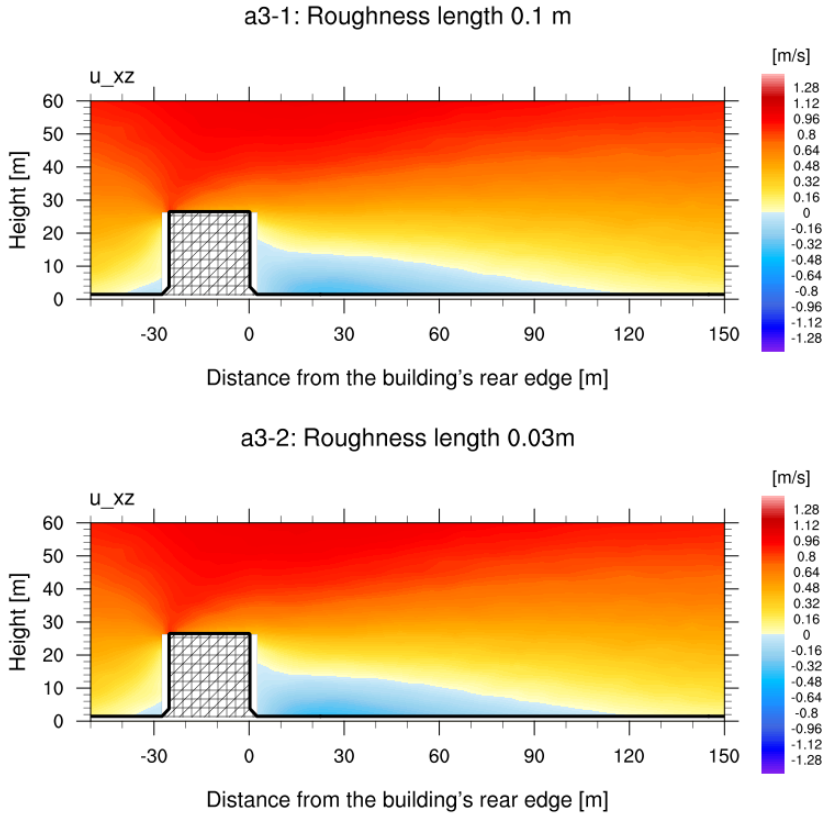


Figure 4.10: Horizontally averaged xz-section of $u$ (m/s) at $t = 288000$ s for roughness values of $z_0 = 0.10$ m and $z_0 = 0.03$ m.

### 4.3.5 Test case a3-1: advection, turbulence

In the test cases a3-1 and a3-2, the length of the wake vortex should be checked depending on the boundary layer turbulence. First, in test case a3-1, the length of the wake should be compared with the analytical solution, where the length must be between $4 \cdot$ H and $5 \cdot$ H. This test case is to be performed with the simulation results of a1-2. Therefore, the length of the wake must be between 100 m and 125 m. If this criterion is fulfilled, the test case is considered passed.

The upper graph in Fig. 4.10 shows the vertical section of the $u$-component, averaged in the $y$-direction. To determine the length of the wake vortex, it is checked up to which distance from the building negative wind speeds occur. The maximum distance from the building finally indicates the length of the wake. In this case, the vortex length is

123.83 m. This fulfills the criterion described above.
⇒ **Test case passed**

### 4.3.6 Test case a3-2: advection, turbulence

In test case a3-2 it should be checked whether a lower roughness length leads to a higher extension of the wake vortex. For this purpose, the simulation from test case a3-1 is repeated with $z_0 = 0.003$ m.
The wake vortex is visible in the lower graph of Fig. 4.10. The vortex increases from 123.83 m to 125.18 m. Thus, the test case a3-2 is passed.
⇒ **Test case passed**

| building | |
|---|---|
| building dimensions | $H = 25$ m<br>$L = 25$ m<br>$B = 25$ m |
| position of the centre: | $x = 0$ m, $y = 0$ m |
| **simulation parameter** | |
| simulation period: | 2 hours |
| averaging period: | 1 hour |
| **meteorology** | |
| wind direction: | 270° |
| wind speed at $P_{Norm}$: | 1 m/s |
| pressure gradient: | $D_x = -0.000017$ Pa/m, $D_y = 0.0$ Pa/m |
| Coriolis force: | no |
| **further parameter** | |
| roughness: | ground: 0.1 m, walls 0.01 m |
| normalization point $P_{Norm}$: | $x = -62.5$ m, $y = 0$ m, $z = 75$ m |

Table 4.5: Input parameters of test case a4-1

### 4.3.7 Test case a4-1: symmetry

In this test case, the symmetry of the simulation results is tested. For this purpose, the building from test case a1-2 is bounded in the $y$-direction with $B = 25$ m. Table 4.5 lists the other input parameters. The permitted difference are $W = 0.01$ m/s and $D = 0.05$. The hit rate must not fall below the 95 % limit.
The quantities $u$, $w$ and $K_m$ are compared in the test. Each grid point $P_i(x_i, y_i, z_i)$ with $y_i > 0$ m is compared with the symmetrical point $P_i'(x_i, -y_i, z_i)$ with $y_i < 0$ m. The hit rates for $u$ are at 99.68 %, for $w$ at 99.85 % and for $K_m$ at 99.84 %.
⇒ **Test case passed**

### 4.3.8 Test case a4-2: effect of the grid spacing

The influence of the grid spacing is tested in test case a4-2. Therefore the test case a4-1 is carried out with a grid spacing of 1.25 m. The used grid parameters are listed in table 4.6
Figure 4.11 shows the horizontally distributions of the $u$-component for both cases. A similar distribution pattern can be seen. For the comparison, the standardized model results from test case a4-2 are aggregated on the coarser grid of a4-1. The hit rate of the individual wind components $u$, $v$ and $w$ should be over 95 %. In the comparison, the grid points of the near field are considered. The near field extends $1 \cdot$ H on the

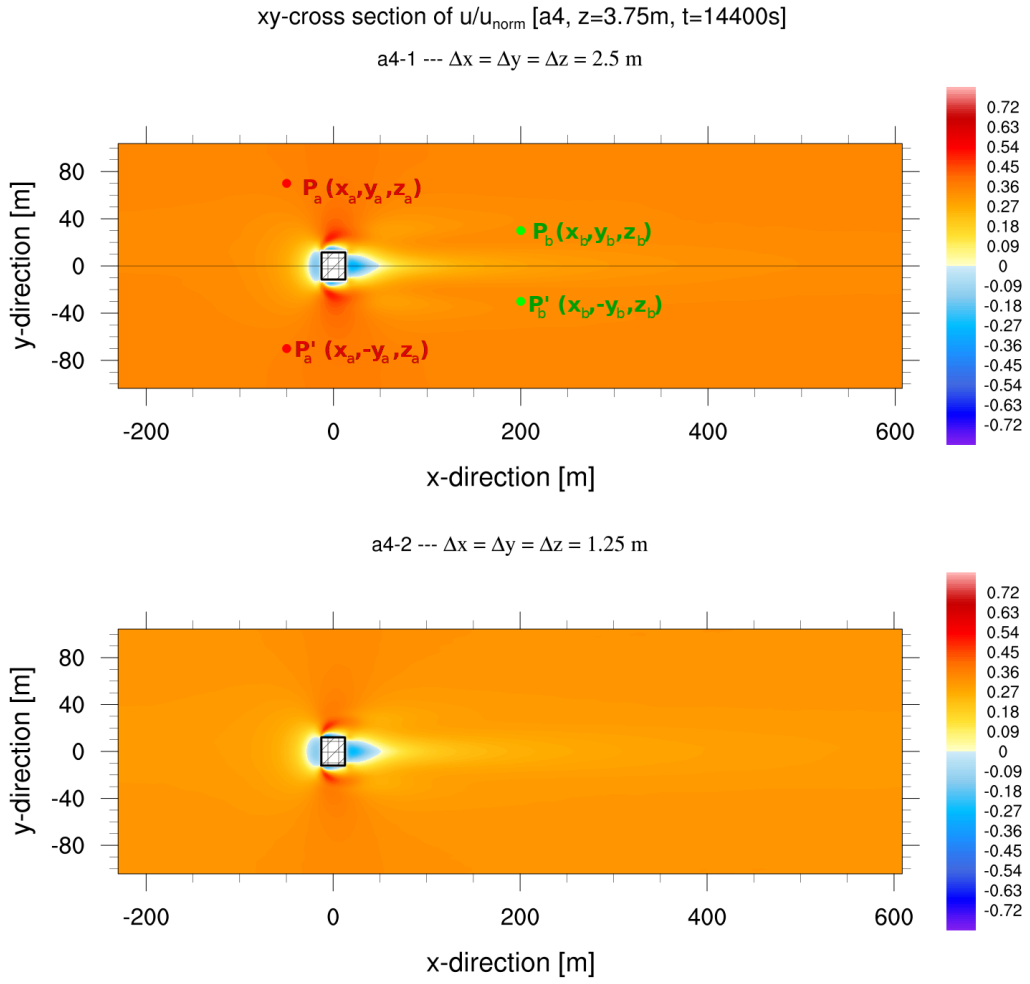


Figure 4.11: xy-sections of $u/u_{norm}$ for $k = 1$ at $t = 21600$ s at a grid resolution of 2.5 m (top) and 1.25 m (bottom).

| model area | |
|---|---|
| grid points | $nx = 671$<br>$ny = 167$<br>$nz = 80$ |
| grid spacing | $dx = 1.25$ m<br>$dy = 1.25$ m<br>$dz = 1.25$ m (for $z \leq 37.5$ m)<br>$dz_{k+1} = dz_k \cdot 1.08$ (for $z > 37.5$ m)<br>$dz_{max} = 20$ m |
| extension | $-230$ m $\leq x \leq 608.75$ m<br>$-105$ m $\leq y \leq 103.75$ m<br>0 m $\leq z \leq 589.46$ m |

Table 4.6: Input parameters of test case a4-2

windward side of the building, $2 \cdot$ H in the lee, $0.5 \cdot$ H in width and $1.5 \cdot$ H in height. The calculated hit rate is 95.32 % for the $u$-component, 99.61 % for the $v$-component and 99.42 % for the vertical component of the wind.
$\Rightarrow$ **Test case passed**

### 4.3.9 Test case a5: building alignment in the grid

In the test case a5, the dependence of the model results on the building alignment in the grid is to be tested. It is required that with a horizontal resolution of 2.5 m the model results have a match of 66 % with different building alignments in the grid.
To test this property, two simulations are preformed. In the first simulation a5-1, the building is aligned parallel to the coordinate axis. The direction of flow is 225°. In the second simulation a5-2, the building is rotated by 45° to the coordinate axis. The flow is 270°. The wind speed in both cases is 1 m/s at the normalization point. In test case a5-1 the normalization point is at $x$ = -44.19 m, $y$ = -44.19 m and $z$ = 50 m. In test case a5-2 the simulation results are normalized with the values at $x$ = -62.49 m, $y$ = 0 m and $z$ = 50 m. The other input parameters are listed in table 4.7.
To evaluate the results, the model results from test case a5-2 are transformed to the grid of a5-1. For this purpose, the grid is rotated by the angle $\varphi$ = 45 °. For the rotated coordinates $x'$ and $y'$

$$\begin{aligned} x' &= xcos\varphi + ysin\varphi \\ y' &= ycos\varphi - xsin\varphi \end{aligned} \tag{4.9}$$

apply. Likewise, the transformed wind components $u'$ and $v'$ are calculated:

$$\begin{aligned} u' &= ucos\varphi + vsin\varphi \\ v' &= vcos\varphi - usin\varphi \ . \end{aligned} \tag{4.10}$$

Figure 4.12 outlines the different simulation grids and flow directions of the two test cases. Since the grid points of the rotated grid (shown in red) are not positioned on the grid points of the simulation grid of test case a5-1 (shown in black), the values of $u'$ and $v'$ must be interpolated to the grid points of a5-1. However, in this case an interpolation is only necessary in the horizontal (bilinear interpolation). The relative distances $x_d$ and $y_d$ of the point P to the grid points of the transformed grid, which are required for the interpolation, can not be determined according to equation 4.5 due to the rotation of the grid.
To determine the distances, simple trigonometric relationships are used. First, the grid cell of the transformed grid (red) is divided into four triangles (see Fig. 4.13).
Depending on the position of the point P in the four areas, the distances $a$ and $b$ are determined (see Fig. 4.14):

$$\begin{aligned} a &= x - x'_{icorn,jcorn} \\ b &= y - y'_{icorn,jcorn} \end{aligned} \tag{4.11}$$

| | |
|---|---|
| **model area** | |
| grid points | $nx = 356$<br>$ny = 383$<br>$nz = 64$ |
| grid spacing | $dx = 2.5$ m<br>$dy = 2.5$ m<br>$dz = 2.5$ m (for $z \leq 37.5$ m)<br>$dz_{k+1} = dz_k \cdot 1.08$ (for $z > 37.5$ m)<br>$dz_{max} = 20$ m |
| extension | $-162.5$ m $\leq x \leq 730$ m<br>$-162.5$ m $\leq y \leq 797.5$ m<br>0 m $\leq z \leq 714.5973$ m |
| **building** | |
| building dimensions<br><br><br>position of the centre: | $H = 25$ m<br>$L = 25$ m<br>$B = 25$ m<br>$x = 0$ m, $y = 0$ m |
| **simulation parameter** | |
| simulation period:<br>averaging period: | 8 hours<br>2 hour |
| **meteorology** | |
| wind direction:<br>wind speed at $P_{Norm}$:<br>pressure gradient:<br><br>Coriolis force: | 225° (a5-1), 270° (a5-2)<br>1 m/s<br>$D_x = -0.0000056$ Pa/m, $D_y = 0.0000056$ Pa/m (a5-1)<br>$D_x = -0.000008$ Pa/m, $D_y = 0.0000$ Pa/m (a5-2)<br>no |
| **further parameter** | |
| roughness: | ground: 0.1 m, walls 0.01 m |

Table 4.7: Input parameters of test case a1-1

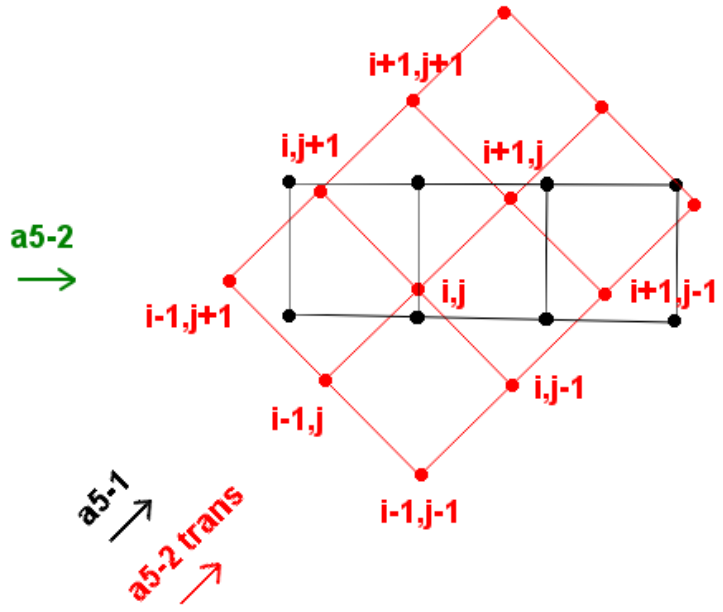


Figure 4.12: Sketch for alignment of the grid in test case a5-1 and of the transformed grid in case a5-2.

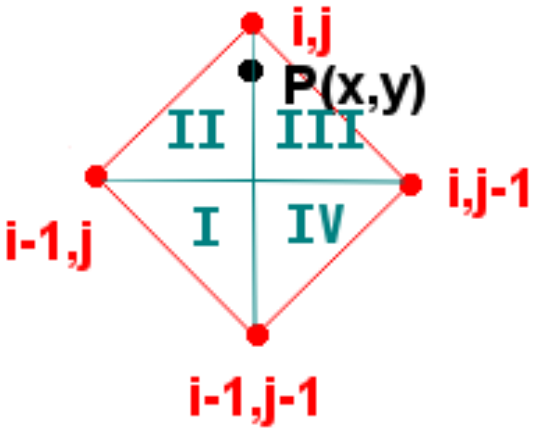


Figure 4.13: Sketch for dividing the grid area into four areas.

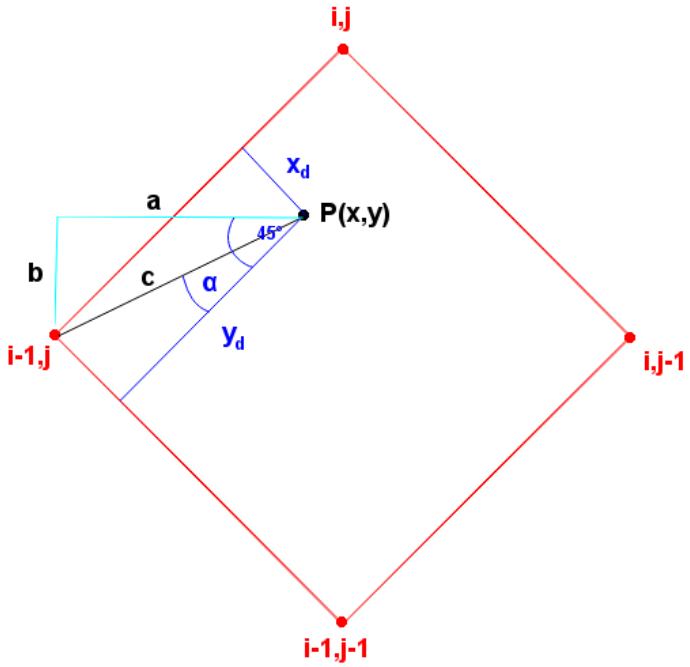


Figure 4.14: Sketch for calculating $x_d$ and $y_d$.

with

$$(icorn, jcorn) = \begin{cases} (i, j) & \text{for triangle I} \\ (i-1, j) & \text{for triangle II} \\ (i-1, j-1) & \text{for triangle III} \\ (i, j-1) & \text{for triangle IV} \end{cases} \tag{4.12}$$

Using the distance $c$, which describes the distance of the point $P$ to the grid point defined in equation 4.12

$$c = \sqrt{a^2 + b^2} \ , \tag{4.13}$$

and the angle $\alpha$

$$\alpha = 45^\circ - \arcsin\left(\frac{b}{c}\right) \tag{4.14}$$

result the relative distances $x_d$ and $y_d$ for triangle II and triangle III

$$x_d = \frac{c \cdot \sin(\alpha)}{2.5\text{m}}, \quad y_d = \frac{c \cdot \cos(\alpha)}{2.5\text{m}} \tag{4.15}$$

and for triangle I and IV

$$x_d = 1 - \frac{c \cdot \sin(\alpha)}{2.5\text{m}}, \quad y_d = 1 - \frac{c \cdot \cos(\alpha)}{2.5\text{m}} \ . \tag{4.16}$$

Analogous to equation 4.6, the meteorological fields are interpolated to the points of the grid of test case a5-1. It should be noted, that the default value is passed on during interpolation in the area of the building. For this reason, in the transformed and interpolated field of test case a5-2 the range with default values increases (see Fig. 4.15, below).
In this test case, all three wind components and the diffusion coefficient are compared. Figure 4.15 shows the xy section of the normalized wind velocity component $u$ for both simulations. It is a good match to recognize, which is also reflected in the other levels, so that the hit rate for the $u$-component is 99.52 %. The permitted differences are $W =$ 0.06 m/s and $D = 0.25$ For the $v$ component, the matching of the simulation results is 99.35 %, for $w$ 99.70 % and for $K_m$ 99.70 %.
⇒ **Test case passed**

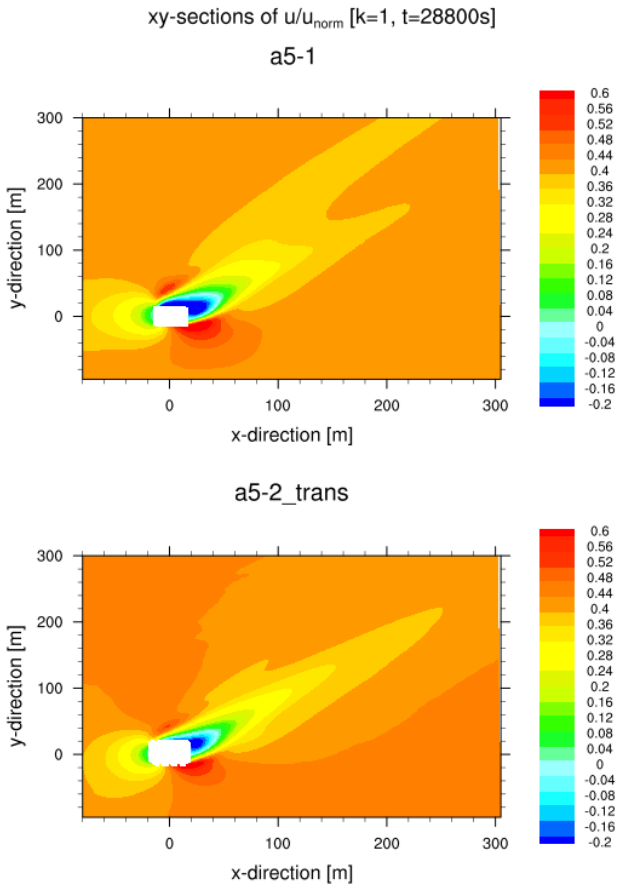


Figure 4.15: xy-sections of $u/u_{norm}$ at $k = 1$ for $t = 28800$ s of the test case a5-1 (top) and the transformed and interpolated field of test case a5-2 (below).

| model area | |
|---|---|
| grid points | $nx = 35$<br>$ny = 35$<br>$nz = 126$ |
| grid spacing | $dx = 2$ m<br>$dy = 2$ m<br>$dz = 2$ m |
| extension | $-35$ m $\leq x \leq 35$ m<br>$-35$ m $\leq y \leq 35$ m<br>0 m $\leq z \leq 253$ m |
| **simulation parameter** | |
| simulation period:<br>averaging period: | 60 hours<br>2 hour |
| **meteorology** | |
| wind direction:<br>wind speed at $P_{Norm}$:<br>pressure gradient:<br>Coriolis force: | $0^\circ$<br>1 m/s<br>$D_x = -0.0$ Pa/m, $D_y = 0.0000095$ Pa/m<br>no |
| **further parameter** | |
| roughness:<br>normalization point $P_{Norm}$: | ground: 0.1 m<br>$x = 0$ m, $y = 0$ m, $z = 250$ m |

Table 4.8: Input parameters of test case b-1

### 4.3.10 Test case b-1: boundary layer development

In the test case b-1 the horizontal homogeneity should be tested in case of an undisturbed flow (without a building). In addition it should be further investigated whether the calculated wind profile agrees with the analytical solution.
Figure 4.16 shows the horizontally distribution of the $v$-component at 2 m height. The velocity fluctuates in the model area with 0.003 m/s by 1 %, which is reflected in the hit rate of 100 % in terms of the homogeneity with the permitted difference $W = 0.01$ m/s and $D = 0.050$. Likewise for the $u$-component and the diffusion coefficient, the hit rate is 100 %.
For comparison with the analytical solution, the wind profiles of all grid points should be compared with the logarithmic wind profile. For the friction velocity $u_*$ the value of $u_*$ is taken, which is present at the point (0,0,0) in the model results. This value is normalized with the velocity at the normalization point.
The hit rate should be similar to the test for homogeneity above 95 %. Figure 4.17 shows

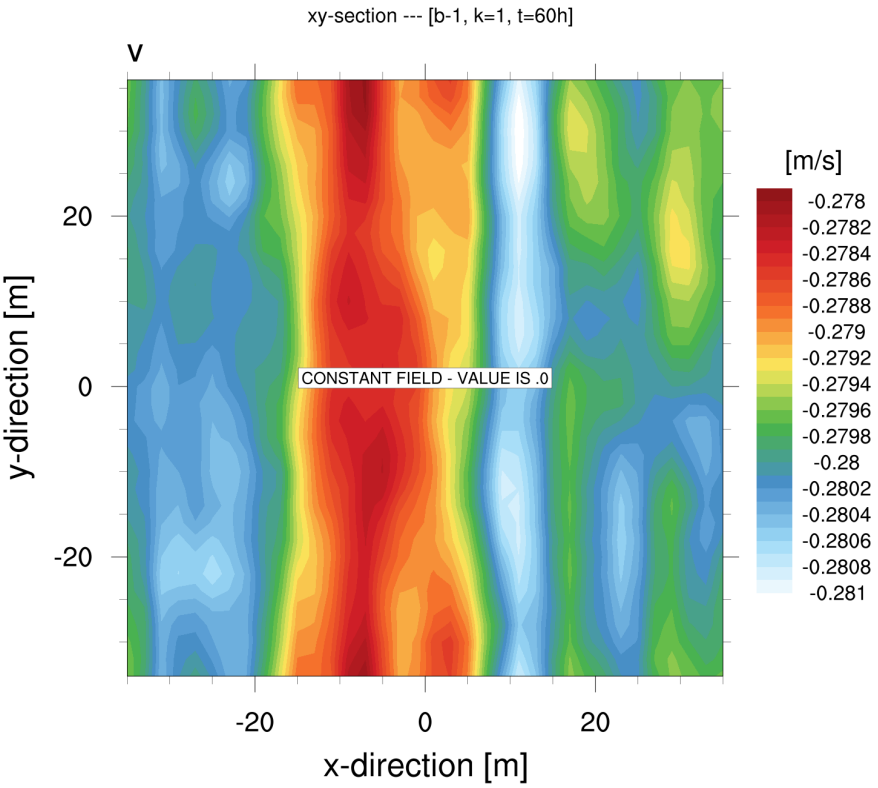


Figure 4.16: xy-section of $v$ (m/s) $k = 1$ and $t = 60$ h for test case b-1.

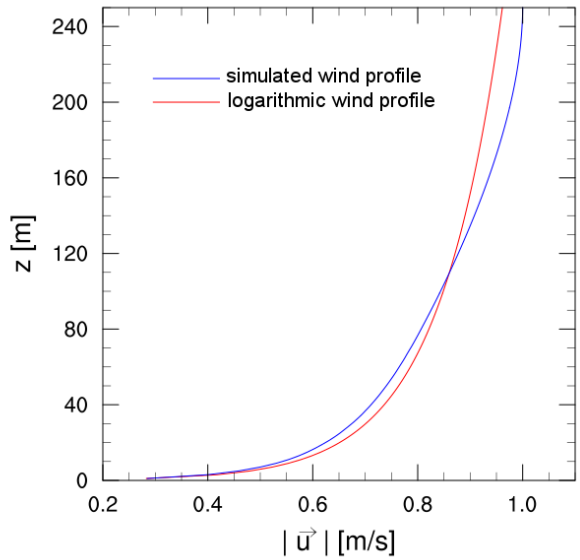


Figure 4.17: Depiction of the analytical wind profile (red) and the simulated wind profile (blue) from test case b-1.

the analytical wind profile (red) and the calculated wind profile (blue) at the point (0,0), which is representative of all calculated wind profiles due to the homogeneity. Both graphs differ in their values at the given differences by less than 1 %. Thus, the test case is passed.

⇒ **Test case passed**

| Test case | wind direction |
|---|---|
| b-2 | 32.3° |
| b-3 | 45° |
| b-4 | 90° |
| b-5 | 180° |
| b-6 | 270° |

Table 4.9: Wind directions of test case b-2 to b-6.

| Test case | homogeneity | | | comparison with b-1 | | |
|---|---|---|---|---|---|---|
| | $u$ | $v$ | $K_m$ | $u$ | $v$ | $K_m$ |
| b-2 | 100 % | 100 % | 100 % | 100 % | 100 % | 100 % |
| b-3 | 100 % | 100 % | 100 % | 100 % | 100 % | 100 % |
| b-4 | 100 % | 100 % | 100 % | 100 % | 99.98 % | 100 % |
| b-5 | 100 % | 100 % | 100 % | 100 % | 100 % | 100 % |
| b-6 | 100 % | 100 % | 100 % | 100 % | 100 % | 100 % |

Table 4.10: Hit rates of test case b-2 to b-6.

### 4.3.11 Test case b-2 to b-6: effect of the approach direction of flow

In this test cases the setup from b-1 is taken. Only the wind direction is varied in the individual test cases (see table 4.9).
The different test cases should show that the model results are independent of the direction of flow. For this purpose, the calculated fields from the test cases b-2 to b-6 are rotated according to the direction of flow and compared with the results from test case b-1. In addition, every result of b-2 to b-6 should also to be checked internally for homogeneity. The profile at the midpoint of the model domain is to be used as a comparison dataset.
The calculated hit rates of the individual test cases are shown in table 4.10. In all cases the hit rate is above 95 %.
⇒ **Test case passed**

| model area | |
|---|---|
| grid points | $nx = 35$<br>$ny = 35$<br>$nz = 160$ |
| grid spacing | $dx = 2$ m<br>$dy = 2$ m<br>$dz = 2$ m (for $z \leq 250$ m)<br>$dz_{k+1} = dz_k \cdot 1.08$ (for $z > 250$ m)<br>$dz_{max} = 20$ m |
| extension | $-35$ m $\leq x \leq 35$ m<br>$-35$ m $\leq y \leq 35$ m<br>0 m $\leq z \leq 613.566$ m |

Table 4.11: Input parameters of test case b-7

### 4.3.12 Test case b-7: effect of the Coriolis force

In this test case, the influence of the Coriolis force on the wind field is tested. For this purpose, the computational grid listed in table 4.11 is used. At the upper edge of the model area Neumann boundary conditions apply for $u$ and $v$. The wind field is initialized via the geostrophic wind on the model surface (with ug_surface = 0 m/s and vg_surface = -1 m/s). The roughness length is 0.1 m. In addition, the Rayleigh damping is applied. This sets the horizontal velocities to the value of their respective basic states (defined by the initial profile). The intensity of the damping is controlled by the Rayleigh factor, which is set to 0.01. The damping begins weakly at a Rayleigh height of 200 m and is increased according to a $\sin^2$ function to a maximum value at the top. It is simulated for 150 hours. The two-hour averaged fields are considered.
Figure 4.18 shows the time course of $E$, $u_*$ and $u_{max}$. After 150 hours stationary conditions are present. The rotation of the wind with the height due to the Coriolis force is shown in Fig. 4.19.
Test case b-7 is passed, if homogeneous conditions are present at all grid points in the model area (hit rate 95 % with W = 0.01 and D = 0.05). In addition, to evaluate the influence of the Coriolis force on the wind direction, the analytically calculated ageostrophic angle $\alpha$ is used

$$\alpha \cong \arcsin\left(\frac{4.3}{\ln(250\text{m}/z_0)}\right) \ . \tag{4.17}$$

With a roughness length of 0.1 m $\alpha = 33.34°$ results. In the simulation without Coriolis force, the wind is rotated relative to the approach direction of flow by only -0.16 ° in 1 m height. With Coriolis force the rotation is -30.91° (see Fig. 4.19). Thus, the numerically solution differs with 30.91 ° less than 10 ° from the analytically solution.

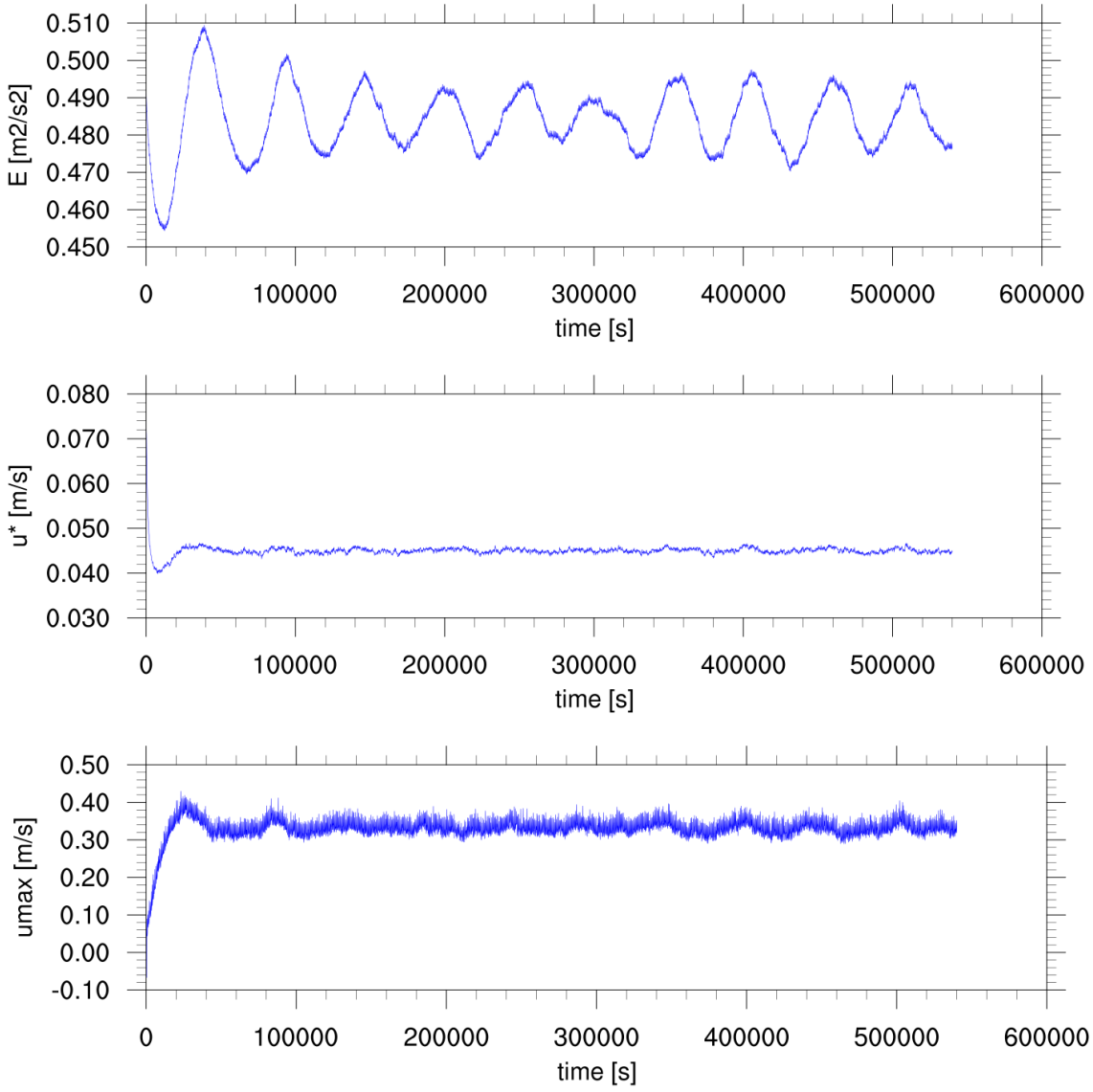


Figure 4.18: Time series of $E$, $u^*$ and $u_{max}$ for test case b-7.

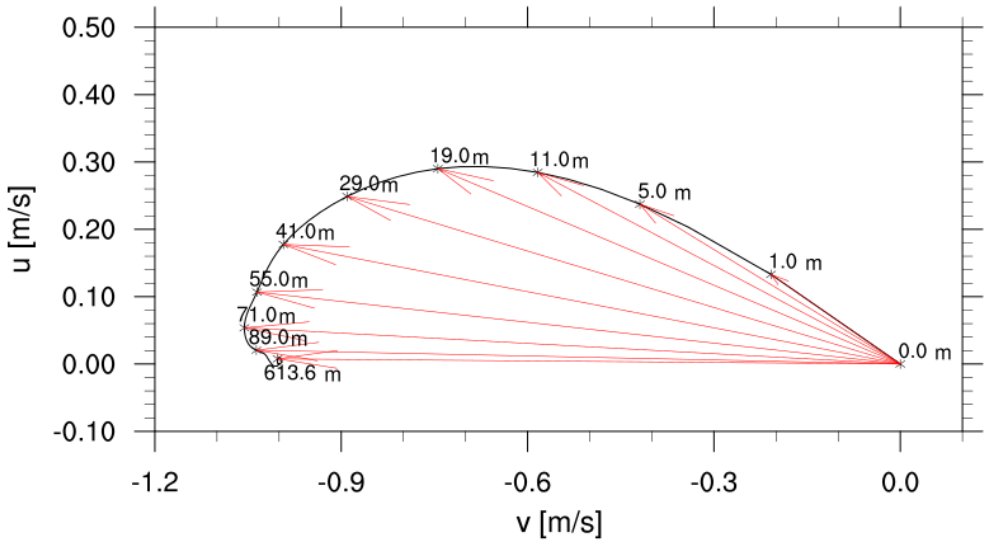


Figure 4.19: Ekman spiral.

⇒ **Test case passed**

| Test case | wind direction |
|---|---|
| b-8 | 32.3° |
| b-9 | 45° |
| b-10 | 90° |
| b-11 | 180° |
| b-12 | 270° |

Table 4.12: Wind directions of test case b-8 to b-12.

| Test case | homogeneity | | | comparison with b-7 | | |
|---|---|---|---|---|---|---|
| | $u$ | $v$ | $K_m$ | $u$ | $v$ | $K_m$ |
| b-8 | 100 % | 100 % | 100 % | 100 % | 99.98 % | 100 % |
| b-9 | 100 % | 100 % | 100 % | 100 % | 100 % | 100 % |
| b-10 | 100 % | 100 % | 100 % | 100 % | 99.94 % | 100 % |
| b-11 | 100 % | 100 % | 100 % | 99.98 % | 99.91 % | 100 % |
| b-12 | 100 % | 100 % | 100 % | 99.99 % | 99.95 % | 100 % |

Table 4.13: Hit rates of test case b-8 to b-12.

### 4.3.13 Test case b-8 to b-12: effect of the Coriolis force and the approach direction of flow

Similarly to test cases b-2 to b-6, different directions of flow are simulated in test cases b-8 to b-12 (see Tab. 4.12). However, in this cases the Coriolis force is considered.
In addition to comparing the meteorology fields with the test case b-7, the quantities $u$, $v$ and $K_m$ should be checked for homogeneity. The hit rates are shown in Tab. 4.13
⇒ **Test case passed**

In the test cases c1 to c5 simulation results are compared with measured values from the wind tunnel. The hit rate must be above 66 % in all cases.

### 4.3.14 Test case c1: advection, turbulence

In test case c1, the results from test case a1-2 are compared with the wind tunnel locations. The comparison takes place at 651 locations in the wind tunnel. The simulation values are interpolated to these locations.
For the successful test case, the hit rate must be at least 66 % with $W = 0.07$ m/s and $D = 0.25$. Compared are the $u$- and $w$-components of the wind.
The calculated hit rate is 81.08 % for the $u$-component and 81.23 % for the $w$-component.
⇒ **Test case passed**

### 4.3.15 Test case c2: advection, turbulence with one building

In test case c2, the results of test case a4-2 are compared with wind tunnel data. The permitted differences are $W = 0.06$ m/s and $D = 0.25$. The three wind components are compared at 870 locations. The hit rate is 88.05 % for $u$, 98.07 % for $v$ and 91.72 % for $w$.
⇒ **Test case passed**

### 4.3.16 Test case c3: approach direction of flow with one building

In this test case, the simulation results from test case a5-1 are compared with wind tunnel measurements.The comparison takes place at 860 locations with $W = 0.06$ m/s and $D = 0.25$. The calculated hit rates are 81.73 % for $u$, 74.79 % for $v$ and 99.70 % for $w$.
⇒ **Test case passed**

### 4.3.17 Test case c4: building width with one building

In test case c4 the flow field around a cuboid building (H = 25 m, L = 20 m and B = 30 m) is considered. The wind is 1 m/s at 43 m altitude. The selected input parameters are shown in Tab. 4.14. The permitted differences are $W = 0.07$ m/s and $D = 0.25$. The $u$-, $v$- and $w$- components are to be compared with values from the wind tunnel at 1134 locations in the range -2·H $\leq x \leq$ 2·H, -1.5·H $\leq y \leq$ 1.5·H and $z \leq$ 4·H.
Figure 4.20 shows the time course of $E$, $u^*$ and $u_{max}$. After about 20 hours stationary conditions are present. The horizontally distribution of wind components is shown in Fig. 4.21.
The calculated hit rates are 85.40 % for $u$, 94.89 % for $v$ and 81.20 % for $w$.
⇒ **Test case passed**

| | |
|---|---|
| **model area** | |
| grid points | $nx = 131$<br>$ny = 83$<br>$nz = 40$ |
| grid spacing | $dx = 2.5$ m<br>$dy = 2.5$ m<br>$dz = 2.5$ m (for $z \leq 37.5$ m)<br>$dz_{k+1} = dz_k \cdot 1.08$ (for $z > 37.5$ m)<br>$dz_{max} = 20$ m |
| extension | $-85$ m $\leq x \leq 242.5$ m<br>$-100$ m $\leq y \leq 107.5$ m<br>0 m $\leq z \leq 236.1362$ m |
| **building** | |
| building dimensions<br><br><br>position of the centre: | $H = 25$ m<br>$L = 20$ m<br>$B = 30$ m<br>$x = 0$ m, $y = 0$ m |
| **simulation parameter** | |
| simulation period:<br>averaging period: | 36 hours<br>2 hour |
| **meteorology** | |
| wind direction:<br>wind speed at $P_{Norm}$:<br>pressure gradient:<br>Coriolis force: | 270°<br>1 m/s<br>$D_x = -0.000034$ Pa/m, $D_y = 0.0$ Pa/m<br>no |
| **further parameter** | |
| roughness:<br>normalization point $P_{Norm}$: | ground: 0.1 m, walls 0.01 m<br>$x = -41.5$ m, $y = 0$ m, $z = 43$ m |

Table 4.14: Input parameters of test case c4

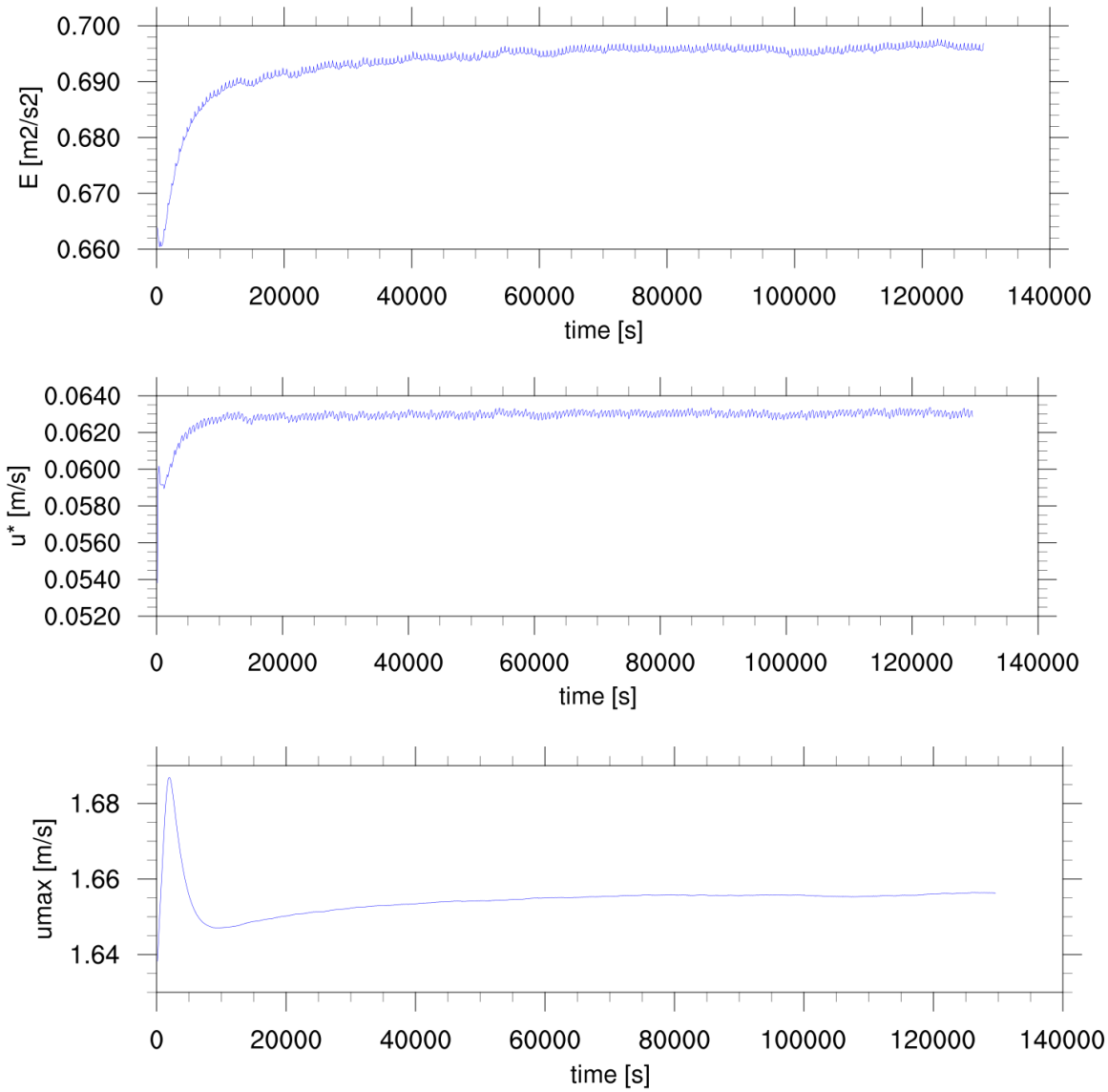


Figure 4.20: Time series of $E$, $u^*$ and $u_{max}$ for test case c4.

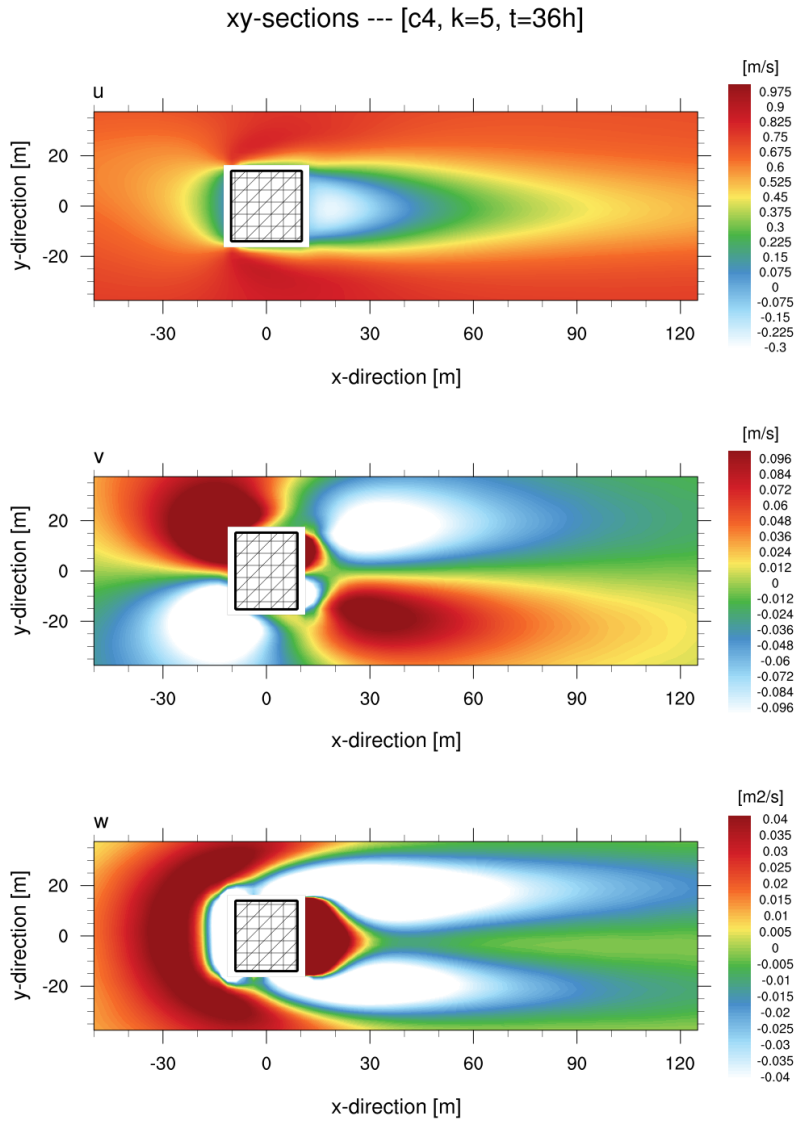


Figure 4.21: xy-sections of $u$ (m/s), $v$ (m/s) and $w$ (m/s) at $k = 5$ and $t = 36$ h for test case c4.

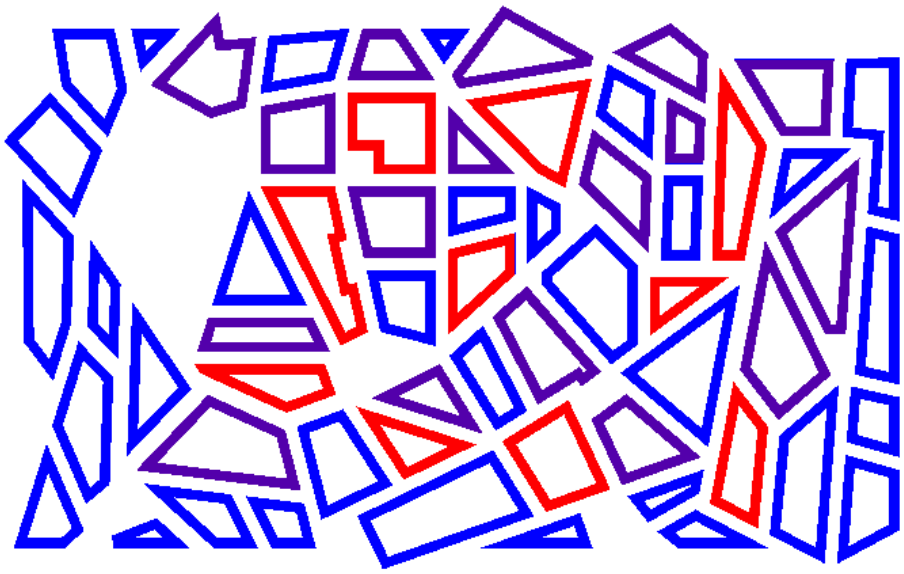

Figure 4.22: Presentation of the buildings of test case c5 (blue: 15 m, purple: 18 m and red: 24 m height).

### 4.3.18 Test case c5: building interaction

In test case c5 the flow in and around a complex building arrangement is examined (see Fig.4.22). The buildings have three different heights. The buildings shown in blue are 15 m high, the purple colored buildings 18 m and the red colored buildings have a height of 24 m. The other input parameters are listed in Tab. 4.15.
In addition to the roughness length of the ground ($z_0$ = 0.1 m) a roughness length between the buildings is indicated in this test case. This length should be 0.034 m. Since it is not clear which area is meant with "between the buildings", two simulations were performed. In the first simulation (called c5-1) the roughness length is set to 0.1 m in the model area. In the second simulation (c5-2) a roughness length of 0.034 m is used. The results of the two different runs are shown in the Figs. 4.23 and 4.24. The upper graphics show the horizontal distribution of the $u$-component respectively $v$-component for c5-1 and the middle graphics the disturbution for c5-2. The deviations can be seen in the lower graphics. They are not greater than the absolute permitted difference of 0.08 m/s. Thus, the error that arises due to the negligence of the roughness length between buildings is acceptable. For comparison with the wind tunnel data the results of c5-1 are used.
In this case, the $u$- and $v$-components of the wind are compared. The hit rate should

| model area | |
|---|---|
| grid points | $nx = 2849$<br>$ny = 1479$<br>$nz = 26$ |
| grid spacing | $dx = 2$ m<br>$dy = 2$ m<br>$dz = 0.6$ m (first level)<br>$dz_{k+1} = dz_k \cdot 1.2$<br>$dz_{max} = 200$ m |
| extension | $-1569$ m $\leq x \leq 4129$ m<br>$-1476$ m $\leq y \leq 1482$ m<br>0 m $\leq z \leq 340.7267$ m |
| **simulation parameter** | |
| simulation period:<br>averaging period: | 6 hours<br>2 hour |
| **meteorology** | |
| wind direction:<br>wind speed at $P_{Norm}$:<br>pressure gradient:<br>Coriolis force: | 270°<br>1 m/s<br>$D_x = -0.000005$ Pa/m, $D_y = 0.0$ Pa/m<br>no |
| **further parameter** | |
| roughness:<br><br>normalization point $P_{Norm}$: | ground: 0.1 m, between building: 0.034 m, walls 0.001 m<br>$x = -450$ m, $y = 0$ m, $z = 110.93$ m |

Table 4.15: Input parameters of test case c5

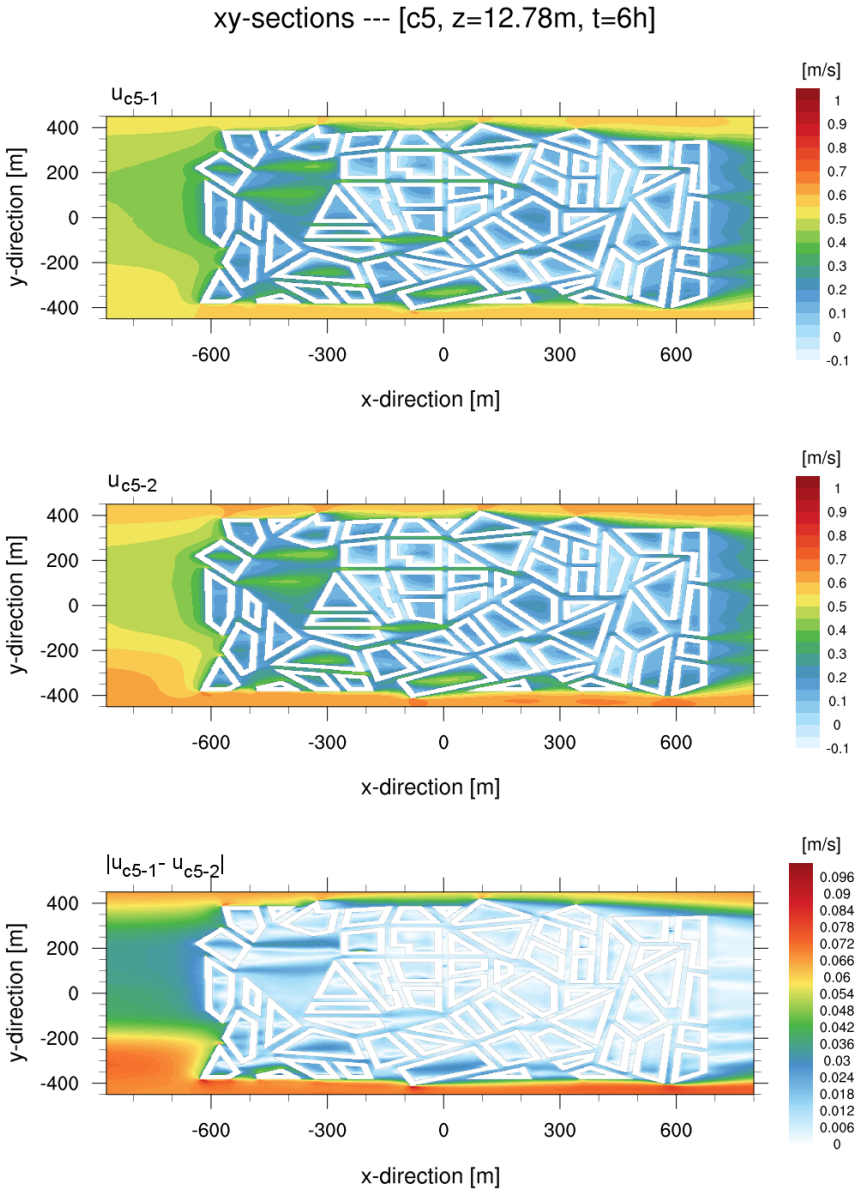


Figure 4.23: xy-sections of $u$ (m/s) at $z = 12.78$ m and $t = 6$ h for test case c5 with $z_0 = 0.1$ m (top) and $z_0 = 0.0034$ m (center). The lower graphic shows the absolute difference.

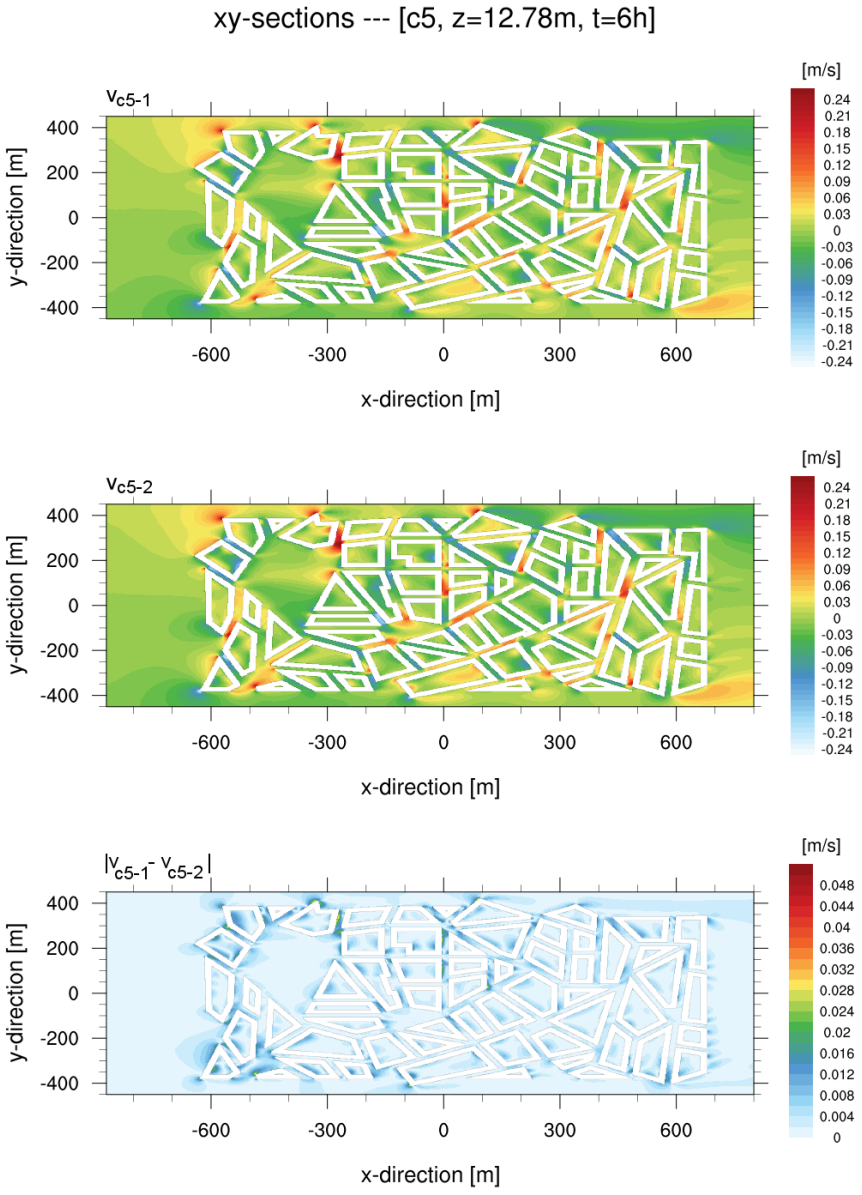


Figure 4.24: xy-sections of $v$ (m/s) at $z = 12.78$ m and $t = 6$ h for test case c5 with $z_0 = 0.1$ m (top) and $z_0 = 0.0034$ m (center). The lower graphic shows the absolute difference.

be above 66 % for the individual components. For simultaneous comparison of the horizontal wind components ($u$,$v$) with the wind tunnel data the hit rate must be greater than 50 %.
The calculated hit rate is 77.85 % for the $u$-component, 87.28 % for the $v$-component and 67.68 % for ($u$,$v$).
⇒ **Test case passed**

# 5 Internal assessment

The evaluation according to VDI 3783 Part 9 includes an automatic execution of the following controls:

- At a control grid point in the interior of the model area $2 \cdot \Delta t$-waves are not to be generated
- The maxima of the standard differences of the meteorological variables are not to be remain at the open edges of the model or travel from there into the interior of the domain with increasing time
- The means of the meteorological variables over the model grid are not to exhibit $2 \cdot \Delta t$-waves or increase or decrease with time (exception: physical cause)
- The mass has to be conserved
- The wind components must be smaller than ten times the maximum wind velocity at the approach flow profile and the potential temperature has to lie between 220 K and 330 K

These controls are contained in `vdi_internal_controls.f90` and can be switched on in the input file via `vdi_checks = .T.`

Model evaluation protocol in conformity with VDI 3783 Part 9
- Required properties -

This document certifies the evaluation of a prognostic microscale wind field model for flow around buildings and obstacles. It conforms to the provisions of VDI 3783 Part 9. Numbers in brackets [ ] refer to the relevant section of the standard. Please complete, crossing out inapplicable items.

| | | |
|---|---|---|
| 0. Particulars of microscale model | PALM , Version 6.0, r4113 | |
| publication date: | Year: 2019 Month: July Day: 23 | |
| person responsible for the model: | Prof. Dr. Siegfried Raasch | |
| person responsible for the evaluation: | Dipl.-Met. Viola Weniger (Institut für Meteorologie und Klimatologie) | |
| address: | Herrenhäuser Str.2, 30419 Hannover | |
| e-mail, tel.: | weniger@muk.uni-hannover.de, 0511/762 2629 | |
| 1. General evaluation | [4.1] | |
| comprehensibility | [4.1.1] | YES / ~~NO~~ |
| brief description | [4.1.2.1] | YES / ~~NO~~ |
| detailed description of the model | [4.1.2.2] | YES / ~~NO~~ |
| user manual | [4.1.2.3] | YES / ~~NO~~ |
| 2. Scientific evaluation | [4.2] | |
| all three wind components are prognostic | [4.2] | YES / ~~NO~~ |
| continuity equation complete or inelastic approximation | [4.2] | YES / ~~NO~~ |
| fluxes continuous as a function of the location | [4.2] | YES / ~~NO~~ |
| fluxes continuous as a function of the stratification | [4.2] | YES / ~~NO~~ |
| direct computation of the near-ground fluxes or wall functions | [4.2] | YES / ~~NO~~ |
| symmetry of the shear tensor | [4.2] | YES / ~~NO~~ |
| buildings resolved explicitly | [4.2] | YES / ~~NO~~ |
| building roughness taken into account | [4.2] | YES / ~~NO~~ |
| 3. Validation | [4.3, E3] | |
| test case a1-1: two-dimensionality | [Table E3] | YES / ~~NO~~ |
| test case a1-2: scalability | [Table E4] | YES / ~~NO~~ |
| test case a2: stationarity | [Table E5] | YES / ~~NO~~ |
| test case a3-1: quasi-2D building/advection, turbulence | [Table E6] | YES / ~~NO~~ |
| test case a3-2: quasi-2D building/advection, turbulence | [Table E7] | YES / ~~NO~~ |
| test case a4-1: symmetry | [Table E8] | YES / ~~NO~~ |
| test case a4-2: effect of grid spacing | [Table E9] | YES / ~~NO~~ |
| test case a5: building alignment in the grid | [Table E10-E11] | YES / ~~NO~~ |
| test case b-1 to b-6: boundary layer, homogeneity, approach direction of flow | [Table E12-E13] | YES / ~~NO~~ |
| test case c1: quasi-2D building/advection, turbulence | [Table E16] | YES / ~~NO~~ |
| test case c2: one building/advection, turbulence | [Table E17] | YES / ~~NO~~ |
| test case c3: one building/approach direction of flow | [Table E18] | YES / ~~NO~~ |
| test case c4: one building/building width | [Table E19] | YES / ~~NO~~ |
| test case c5: building interaction | [Table E20] | YES / ~~NO~~ |
| 4. Model internal controls: | [4.3.3] | |
| Online control: $2\cdot\Delta t$ -wave control point | [4.3] | YES / ~~NO~~ |
| Online control: standard differences | [4.3] | YES / ~~NO~~ |
| Online control: domain averages | [4.3] | YES / ~~NO~~ |
| Online control: conservation of mass | [4.3] | YES / ~~NO~~ |
| Online control: plausible values | [4.3] | YES / ~~NO~~ |

## EVALUATION RESULT

The microscale model PALM , Version 6.0, r4113 is

E V A L U A T E D ~~/ N O T E V A L U A T E D~~

in conformity with VDI 3783 Part 9. The model is deemed evaluated in accordance with VDI 3783 Part 9 if all test points were answered in the affirmative.

I confirm that all the information contained in this certificate was provided to the best of my knowledge and belief. No attempt has been made to modify the model for individual test cases in order to achieve better conformity of the model results with the comparison data.

Hannover, 20.08.2019
(place and date)

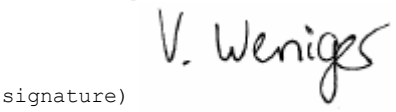

(signature)

Supplement to the model evaluation protocol in conformity with VDI 3783 Part 9
- Application-dependent properties -

This document contains supplementary information for the evaluation of a prognostic microscale wind field model for flow around buildings and obstacles. This supplement conforms to the provisions of VDI 3783 Part 9. Numbers in brackets [ ] refer to the relevant section of the standard. Please complete, crossing out inapplicable items.

| | | |
|---|---|---|
| 0. Supplementary items refer to the model | PALM , Version 6.0, r4113 | |
| publication date: | Year: 2019 Month: July Day: 23 | |
| person responsible for the model: | Prof. Dr. Siegfried Raasch | |
| person responsible for the evaluation: | Dipl.-Met. Viola Weniger (Institut für Meteorologie und Klimatologie) | |
| address: | Herrenhäuser Str.2, 30419 Hannover | |
| e-mail, tel.: | weniger@muk.uni-hannover.de, 0511/762 2629 | |
| 1. General evaluation | | [4.1] |
| disclosure of the source code, technical reference | | [4.1.2.5] YES / ~~NO~~ |
| 2. Scientific evaluation | | [4.2] |
| stratification non-neutral: temperature prognostic | | [4.2] YES / ~~NO~~ |
| stratification non-neutral: specific humidity prognostic | | [4.2] YES / ~~NO~~ |
| stratification non-neutral: buoyancy forces (e.g. Boussinesq approximation) | | [4.2] YES / ~~NO~~ |
| stratification non-neutral: turbulence parameters a function of stability | | [4.2] YES / ~~NO~~ |
| No near-ground winds for initialisation: Coriolis force taken into account | | [4.2] YES / ~~NO~~ |
| terrain gradient > 1:20: orography taken into account explicitly | | [4.2] YES / ~~NO~~ |
| 3D non-equidistant grid | | [4.2] YES / ~~NO~~ |
| 3. Validation | | [4.3, E3] |
| Coriolis force: test case b-7 to b-12: Coriolis force, approach flow | | [Table E14-E15] YES / ~~NO~~ |

## EVALUATION RESULT

The microscale model PALM , Version 6.0, r4113 is

E V A L U A T E D / ~~N O T E V A L U A T E D~~

in conformity with VDI 3783 Part 9. The model is deemed evaluated in accordance with VDI 3783 Part 9 if all test points were answered in the affirmative.

I confirm that all the information contained in this certificate was provided to the best of my knowledge and belief. No attempt has been made to modify the model for individual test cases in order to achieve better conformity of the model results with the comparison data.

Hannover, 20.08.2019 V. Weniger

(place and date) (signature)

# Bibliography

**Gronemeier, T., M. Sühring, 2019:** On the Effects of Lateral Openings on Courtyard Ventilation and Pollution  a Large-Eddy Simulation Study. — *Atmosphere*, **10(2)**, 63.

**Kanani-Sühring, F., S. Raasch, 2017:** Enhanced scalar concentrations and fluxes in the lee of forest patches: a large-eddy simulation study. — *Boundary-Layer Meteorol.*, **164(1)**, 1–17.

**Knoop, H., F. Ament, B. Maronga, 2019:** A generic gust definition and detection method based on wavelet-analysis. — *Advances in Science and Research*, submitted.

**Kolmogorow, A. N., 1942:** Equations of turbulent motion of an incompressible fluid. — *Izv. Akad. Nauk SSSR Ser. Fiz.*, **6**, 56–58.

**Letzel, M. O., 2007:** *High resolution Large-Eddy Simulation of turbulent flow around buildings.* — Dissertation, Gottfried Wilhelm Leibniz Universität Hannover.

**Maronga, B., S. Banzhaf, C. Burmeister, T. Esch, R. Forkel, D. Fröhlich, V. Fuka, K. Gehrke, J. Geletic, S. Giersch, T. Gronemeier, G. Gro, W. Heldens, A. Hellsten, F. Hoffmann, A. Inagaki, E. Kadasch, F. Kanani-Sühring, K. Ketelsen, B. A. Khan, C. Knigge, H. Knoop, P. Krc, M. Kurppa, H. Maamari, A. Matzarakis, M. Mauder, M. Pallasch, D. Pavlik, J. Pfafferott, J. Resler, S. Rissmann, E. Russo, M. Salim, M. Schrempf, J. Schwenkel, G. Seckmeyer, S. Schubert, M. Sühring, R. von Tils, L. Vollmer, S. Ward, B. Witha, H. Wurps, J. Zeidler, S. Raasch, 2019:** Overview of the PALM model system 6.0. — *Geosci. Model Dev. Discuss.*, submitted.

**Maronga, B., M. Gryschka, R. Heinze, F. Hoffmann, F. Kanani-Sühring, M. Keck, K. Ketelsen, M. O. Letzel, M. Sühring, S. Raasch, 2015:** The Parallelized Large-Eddy Simulation Model (PALM) version 4.0 for Atmospheric and Oceanic Flows: Model Formulation, Recent Developments, and Future Perspectives. — *Geosci. Model Dev.*, **8**, 2515–2551.

**Prandtl, L., 1945:** *Über ein neues Formelsystem für die ausgebildete Turbulenz.* — Nachr. Ges. Wiss. Göttingen. Math.-Phys. Kl., 6-9 S.

**Schwenkel, J., B. Maronga, 2019:** Large-eddy simulation of radiation fog with comprehensive two-moment bulk microphysics: Impact of different aerosol activation and condensation parameterizations. — *Atmos. Chem. Phys. Discuss.*, in review.

**VDI 3783 Bl. 12, 2000:** *Umweltmeteorologie. Physikalische Modellierung von Strömungs- und Ausbreitungsvorgängen in der atmosphärischen Grenzschicht. Windkanalanwendungen.* — Beuth Verlag, 33 pp.

**VDI 3783 Bl. 9, 2017:** *Umweltmeteorologie. Prognostische mikroskalige Windfeldmodelle. Evaluierung für Gebäude- und Hindernisumströmung.* — Beuth Verlag, 68 pp.